

Search for new phenomena in events with at least three photons collected in pp collisions at $\sqrt{s} = 8$ TeV with the ATLAS detector

ATLAS Collaboration*

CERN, 1211 Geneva 23, Switzerland

Received: 17 September 2015 / Accepted: 25 March 2016 / Published online: 16 April 2016

© CERN for the benefit of the ATLAS collaboration 2016. This article is published with open access at Springerlink.com

Abstract Results of a search for new phenomena in events with at least three photons are reported. Data from proton–proton collisions at a centre-of-mass energy of 8 TeV, corresponding to an integrated luminosity of 20.3 fb^{-1} , were collected with the ATLAS detector at the LHC. The observed data are well described by the Standard Model. Limits at the 95 % confidence level on new phenomena are presented based on the rate of events in an inclusive signal region and a restricted signal region targeting the rare decay $Z \rightarrow 3\gamma$, as well as di-photon and tri-photon resonance searches. For a Standard Model Higgs boson decaying to four photons via a pair of intermediate pseudoscalar particles (a), limits are found to be $\sigma \times \text{BR}(h \rightarrow aa) \times \text{BR}(a \rightarrow \gamma\gamma)^2 < 10^{-3} \sigma_{\text{SM}}$ for $10 \text{ GeV} < m_a < 62 \text{ GeV}$. Limits are also presented for Higgs boson-like scalars (H) for $m_H > 125 \text{ GeV}$, and for a Z' decaying to three photons via $Z' \rightarrow a + \gamma \rightarrow 3\gamma$. Additionally, the observed limit on the branching ratio of the Z boson decay to three photons is found to be $\text{BR}(Z \rightarrow 3\gamma) < 2.2 \times 10^{-6}$, a result five times stronger than the previous result from LEP.

1 Introduction

Many extensions of the Standard Model (SM) include phenomena that can result in final states consisting of three or more photons. Extensions of the SM scalar sector [1–5], for example, often include pseudoscalar particles (a) with couplings to the Higgs boson [6, 7] (h) and branching ratios into photons that would be visible at the LHC, in addition to scalars (H) with masses different from the SM-like Higgs boson of $m_h = 125 \text{ GeV}$ that can also decay via $H \rightarrow aa \rightarrow 4\gamma$. Other models feature additional vector gauge bosons that can decay to a photon and a new pseudoscalar boson, a , with the subsequent decay of the a into a pair of photons, resulting in a three-photon final state [8]. Moreover, in the SM, the Z boson can decay to three pho-

tons via a loop of W^\pm bosons or fermions. The decay is heavily suppressed and the branching ratio is predicted to be $\sim 5 \times 10^{-10}$ [9]. The current most stringent bound on this process comes from the L3 Collaboration, which placed a limit of $\text{BR}(Z \rightarrow 3\gamma) < 10^{-5}$ [10]. The ATLAS detector has collected $\sim 10^9$ Z boson events, and thus an observation of this decay would indicate an enhancement of this decay rate and could be evidence of phenomena not predicted by the SM. Feynman diagrams for some of these beyond-the-Standard Model (BSM) and rare SM scenarios are shown in Fig. 1.

To ensure sensitivity to these and other possible rare SM and BSM scenarios, an inclusive three-photon search is performed using 20.3 fb^{-1} of LHC proton–proton collisions collected by the ATLAS detector in 2012 at a centre-of-mass energy of 8 TeV. Such a model-independent search is the first of its kind, as are the interpretations for a Higgs boson decaying to four photons via two intermediate pseudoscalar a particles (for a Higgs boson of $m_h = 125 \text{ GeV}$ and for Higgs-like scalars of higher masses) and for three-photon resonances corresponding to a new vector gauge boson.

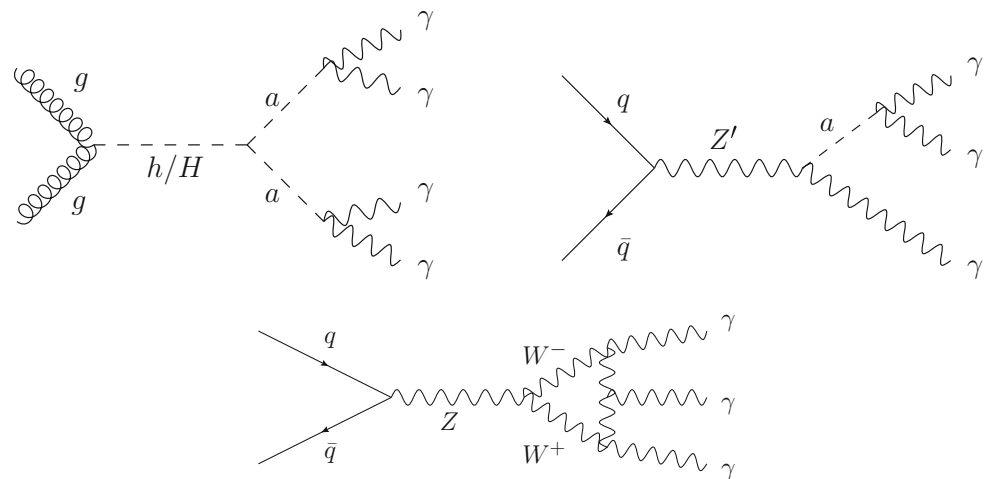
The dominant backgrounds include the irreducible component with three or more prompt photons, as well as the reducible components consisting of combinations of photons and electrons or hadronic jets misidentified as photons. The contributions from events with jets which are misidentified as photons are calculated from data-driven methods, while simulation is used to estimate the contributions from the irreducible background and the reducible background originating from electroweak processes that lead to electrons which are misidentified as photons in the detector. Collision data is used to derive corrections to the probability obtained from simulation that electrons are misidentified as photons.

2 The ATLAS detector

The ATLAS experiment [11] at the LHC is a multi-purpose particle detector with a forward-backward symmetric cylin-

* e-mail: atlas.publications@cern.ch

Fig. 1 Feynman diagrams for possible beyond-the-Standard Model (*top*) and rare Standard Model (*bottom*) scenarios that result in final states with at least three photons



dric geometry and a near 4π coverage in solid angle.¹ It consists of an inner tracking detector surrounded by a thin superconducting solenoid providing a 2 T axial magnetic field, electromagnetic (EM) and hadronic calorimeters, and a muon spectrometer. The inner tracking detector covers the pseudorapidity range $|\eta| < 2.5$. It consists of silicon pixel, silicon micro-strip, and transition radiation tracking detectors. Lead/liquid-argon (LAr) sampling calorimeters provide EM energy measurements with high granularity. A hadronic (iron/scintillator-tile) calorimeter covers the central pseudorapidity range ($|\eta| < 1.7$). The end-cap and forward regions are instrumented with LAr calorimeters for both EM and hadronic energy measurements up to $|\eta| = 4.9$. The muon spectrometer surrounds the calorimeters and is based on three large air-core toroid superconducting magnets with eight coils each. Its bending power ranges from 2.0 to 7.5 T m. It includes a system of precision tracking chambers and fast detectors for triggering. A three-level trigger system is used to select events. The first-level trigger is implemented in hardware and uses a subset of the detector information to reduce the accepted rate to at most 75 kHz. This is followed by two software-based trigger levels that together reduce the accepted event rate to 400 Hz on average depending on the data-taking conditions during 2012.

3 Event and object selection

This search utilises a three-photon trigger that places a minimum requirement on the photon momentum in the plane

¹ ATLAS uses a right-handed coordinate system with its origin at the nominal interaction point (IP) in the centre of the detector and the z -axis along the beam pipe. The x -axis points from the IP to the centre of the LHC ring, and the y -axis points upwards. Cylindrical coordinates (r, ϕ) are used in the transverse plane, ϕ being the azimuthal angle around the beam pipe. The pseudorapidity is defined in terms of the polar angle θ as $\eta = -\ln \tan(\theta/2)$.

transverse to the beam axis (transverse momentum, or p_T) of 15 GeV, applied on three photon candidates in the EM calorimeter. Each candidate is additionally required to satisfy a set of *loose* photon identification criteria [12]. Stringent detector and data quality criteria are applied offline. Events are required to contain at least one interaction vertex, with no additional vertex requirements.

Photon candidates must satisfy a pseudorapidity requirement of $|\eta| < 2.37$, excluding the transition region between the barrel and end-cap of $1.37 < |\eta| < 1.52$, and must satisfy requirements on the shape of the energy deposit in the calorimeter. A photon candidate is rejected if the barycentre of its energy deposit is within a cone of $\Delta R \equiv \sqrt{(\Delta\eta)^2 + (\Delta\phi)^2} < 0.15$ around the barycentre of the energy deposit of a higher p_T photon candidate. Finally, selected photon candidates are required to satisfy a more stringent set of identification criteria, known as *tight* [12]. Photon isolation is defined by the amount of transverse energy, E_T^{iso} , deposited in the EM calorimeter within a cone of size ΔR around the photon candidate, excluding the energy of the photon candidate itself. It is a powerful means of distinguishing between photons and hadronic jets misidentified as photons, since the energy clusters deposited by photons in the EM calorimeter tend to be narrower in the transverse direction than those deposited by jets. Because minimum-bias proton–proton interactions in the same or nearby bunch crossings (pileup) can affect the calculated photon isolation energy, a correction is applied based on an event-by-event energy density pileup estimation. This search uses an isolation cone of size $\Delta R < 0.4$, and a correction to the E_T^{iso} value of a photon candidate is made when another photon candidate passing the *tight* identification criteria is found within an annulus of $0.15 < \Delta R < 0.4$ around the photon candidate. The correction consists of subtracting the p_T value of the other photon candidate found within the annulus from the E_T^{iso} value of the photon candidate under consideration. The final isolation criterion is $E_T^{\text{iso}} < 4$ GeV.

Events in the inclusive signal region are required to have at least three tightly identified and isolated photon candidates, where the two photon candidates with the highest transverse momentum must have $p_T > 22$ GeV while the third highest must have $p_T > 17$ GeV. The restricted signal region, targeting the rare decay $Z \rightarrow 3\gamma$, is a subset of these events where an additional criterion of $80 \text{ GeV} < m_{3\gamma} < 100 \text{ GeV}$ is placed on the invariant mass of the three-photon system. The signal regions are supplemented by several control regions, where at least one of the photon candidates fails the isolation requirement.

4 Simulated event samples

Simulated event samples are used to estimate several SM background processes in the search for excesses in the inclusive signal regions, as well as to model signal predictions for both the inclusive searches and the resonance searches for the specific BSM scenarios considered here. The simulated BSM signal samples are also used to define a fiducial region for which the search criteria are largely model-independent.

4.1 Simulated backgrounds

The SM two-photon process is an irreducible background to a three-photon search because a third photon may arise from minimum-bias proton–proton interactions in the same bunch crossing. The SM two-photon background is simulated with PYTHIA 8 [13], and the three- and four-photon backgrounds are simulated with MADGRAPH 5 [14], with PYTHIA 8 used for fragmentation and hadronisation. The production of two, three and four photons in the SM contains large contributions from higher-order Feynman diagrams. Thus, the two-, three- and four-photon simulated event samples calculated at leading order (LO) are multiplied by factors (“ K -factors”) determined from studies with generators that include next-to-leading order (NLO) contributions, namely MCFM 6.8 [15] and VBFNLO 2.7.0 [16–18], using the parton distribution function (PDF) sets CTEQ6L1 [19] for the LO cross sections and CT10 [20] and MSTW8NL [21] for the NLO cross sections. These K -factors are 1.9 ± 0.2 for the two-photon process and 3.3 ± 0.5 for the three-photon process. The four-photon process is not included in NLO generators, and since the four-photon background is $\sim 10^{-3}$ of the total background expectation in the inclusive signal region, the three-photon K -factor is applied to the four-photon background sample. The uncertainties for these K -factors are determined by multiplying the renormalisation and factorisation scales independently by 2 and 0.5 and taking the largest deviations from the nominal value of the K -factor.

The reducible backgrounds where electrons are misidentified as photons originate from multiple sources. Processes

where a Z boson decays to an e^+e^- pair, accompanied by a photon not from the matrix element, are modelled with POWHEG-BOX 1.0 [22], using PYTHIA 8 for fragmentation and hadronisation, and $Z+\gamma$ production is modelled with SHERPA 1.4.1 [23]. Backgrounds from processes involving the leptonic decay of the W boson in association with photons and/or hadronic jets are simulated with ALPGEN [24] and HERWIG [25,26]. Possible mis-measurement of the rate of electrons misidentified as photons in simulation is addressed by comparing to electrons misidentified as photons from $Z \rightarrow e^+e^-$ events in data.

To obtain estimates of the rates at which true photons populate the regions of kinematic phase space assumed to be dominated by jets (used in the calculation of the systematic uncertainty for the data-driven estimate of jet backgrounds), a sample containing events with one hard-process quark or gluon and one prompt photon is simulated using PYTHIA and the CTEQ6L1 PDF set.

The PDF sets for the simulated event samples of background processes used for the final background estimate in the inclusive search, for the MADGRAPH, PYTHIA and ALPGEN + HERWIG samples, are taken from CTEQ6L1, while for the POWHEG-BOX and SHERPA samples the PDF sets are taken from CT10.

4.2 Simulated signal processes

The $Z\gamma\gamma\gamma$ effective vertex has been implemented with FEYNRULES [27,28] and then used in a customised MADGRAPH 5 model which is employed to simulate events, using the CTEQ6L1 PDF set and PYTHIA 8 for fragmentation and hadronisation. Each of the two non-trivial, independent, lowest-order effective Lagrangians for this process [29] contains a dimensionful coupling constant, and the values of these constants have been calculated [30] using the SM expected $Z \rightarrow 3\gamma$ branching ratio of 5.41×10^{-10} . These SM values are used in the simulation. The BSM process of a Higgs boson produced via gluon fusion and decaying to four photons via a pair of intermediate a particles is simulated with POWHEG-BOX and PYTHIA 8 (using the CT10 NLO PDF set). The BSM process of a new vector gauge boson decaying to three photons via $Z' \rightarrow a + \gamma \rightarrow 3\gamma$ is simulated with PYTHIA 8 (using the MSTW2008LO [21] leading-order PDF set).

4.3 Minimum-bias interactions and the ATLAS detector simulation

Minimum-bias proton–proton interactions in the same or nearby bunch crossings (pileup) are modelled with PYTHIA 8, using the MSTW2008LO PDF set. These pileup events are overlaid onto the hard-scattering process for all simulated signal and background samples to reproduce the distribution

of the average number of interactions per bunch crossing observed over the course of data-taking in 2012.

All signal and background samples are processed with the full ATLAS detector simulation [31] based on GEANT 4 [32] and reconstructed using the same software as that used for collision data.

5 Background composition estimate

The backgrounds in the search for excesses in the inclusive signal regions are estimated from a combination of simulated samples (detailed in the previous section) and methods employing collision data. The dominant backgrounds in the inclusive signal region are the irreducible SM two-, three- and four-photon processes, while for the $Z \rightarrow 3\gamma$ search channel, backgrounds involving electrons misidentified as photons are dominant.

5.1 Backgrounds estimated from simulation

The irreducible SM two-, three- and four-photon backgrounds, as well as backgrounds from processes involving electrons in the final state originating from Z decays and those involving the leptonic decay of the W boson in association with photons and/or hadronic jets, are estimated via simulation. The third photon for the SM two-photon background process typically arises from pileup interactions, but can occasionally be a quark- or gluon-initiated jet radiated from the incoming partons which is misidentified as a photon. Possible double-counting with the $2\gamma + 1$ -jet final state (estimated via a data-driven method described in the following section) is avoided by omitting from consideration events in the SM two-photon simulated sample where one of the three photon candidates is a jet, using generator-level information. Possible mis-measurement of the rate of electrons misidentified as photons in simulation is addressed by comparing $Z \rightarrow e^+e^-$ processes in simulation and in data. The per-electron scale factor is the ratio of the misidentification rate determined in data to that determined in simulated samples. This scale factor is independent of p_T and η for the ranges considered here, and is found to be 1.03 ± 0.04 .

5.2 Data-driven estimates of $2\gamma + 1$ -jet, $1\gamma + 2$ -jet, and 3-jet backgrounds

A crucial aspect of the analysis is the data-driven estimate of the backgrounds where hadronic jets are misidentified as photons (hereafter called “jet fakes”), i.e., SM processes that can produce $2\gamma + 1$ -jet, $1\gamma + 2$ -jet, and 3-jet events. Collision data are used to derive efficiencies for photons passing the isolation criterion (ϵ_γ) and rates at which jets are misidentified as isolated photons (f_{jet}). These values of ϵ_γ and f_{jet} are

then used in a likelihood matrix method (described below) to estimate the jet backgrounds.

A sample of photon candidates consisting mainly of jet fakes is defined in the following way. The standard *tight* and *loose* photon identification categories are augmented with a *medium* definition [33], intermediate between *tight* and *loose*. The *medium* photon is defined by relaxing some EM shower shape requirements that provide high levels of rejection of jet fakes. When the *medium* definition is combined with a further requirement that the photon candidates fail *tight* (the combination hereafter called *non-tight*), the result is a sample of photon candidates that is primarily composed of jet fakes. This method presupposes that the E_T^{iso} distribution of the *non-tight* sample is composed primarily of jet fakes, and that the subset of *tight* photons with higher values of E_T^{iso} (the “tail”, here for $E_T^{\text{iso}} > 7$ GeV) is dominated by jet fakes. Under these assumptions, the tail of the *non-tight* distribution is scaled to match that of the *tight* distribution, thus providing a determination of the contribution of jet fakes to the signal region, i.e., the collection of photons that pass both the *tight* and the isolation criteria. The scaled *non-tight* distribution is then subtracted from the *tight* distribution. Photon isolation efficiency, ϵ_γ , is then calculated as the ratio of the number of isolated photons (those that satisfy $E_T^{\text{iso}} < 4$ GeV) to the total number of photons in the *tight* distribution after this subtraction has been performed. The rate at which jet fakes are identified as photons, f_{jet} , is the ratio of the number of isolated photons to the total number of photons in the *non-tight* distribution.

The assumptions described above are validated using simulated samples of events containing photons and jets, described in Sect. 4. Any collection of photon candidates consists of some combination of actual photons, which can be defined as “true”, and other objects that are misidentified as photons. The non-zero true photon contamination in the set of *non-tight* photons, and the set of *tight* photons that fail the isolation criterion, is taken from the simulated samples and is used to derive a systematic uncertainty (described in Sect. 6) on the jet background estimate procedure.

The procedure is performed separately for three kinematic regions as follows. Photons are ordered by p_T , highest to lowest. Three regions in the p_T - η plane are defined as (1) $15 \text{ GeV} < p_T < 40 \text{ GeV}$ and $|\eta| < 1.37$, (2) $p_T > 40 \text{ GeV}$ and $|\eta| < 1.37$, and (3) $1.52 < |\eta| < 2.37$. The separation into lower and higher p_T bins around 40 GeV is chosen because this is the value at which ϵ_γ and f_{jet} are changing rapidly, and the three regions were chosen to maintain a large number of events in each bin. The values of ϵ_γ and f_{jet} are then calculated for each of the three regions, and the results are shown in Table 1.

The data-derived ϵ_γ and f_{jet} values are applied to events with three photon candidates to estimate the SM $2\gamma + 1$ -jet, $1\gamma + 2$ -jet, and 3-jet backgrounds. This is done using a

Table 1 Photon isolation efficiencies (ϵ_γ) and rates of jets misidentified as photons (f_{jet}) from collision data for the three kinematic regions, used for the jet background estimate. The isolation criterion is $E_T^{\text{iso}} <$

4 GeV. The three regions were chosen to maintain a large number of events in each bin. The first uncertainty is statistical while the second is systematic

Kinematic region	Fraction satisfying isolation criterion	
	Photons (ϵ_γ)	Jets misidentified as photons (f_{jet})
1. $15 \text{ GeV} < p_T < 40 \text{ GeV}, \eta < 1.37$	$0.939 \pm 0.007 \pm 0.009$	$0.424 \pm 0.001 \pm 0.013$
2. $p_T > 40 \text{ GeV}, \eta < 1.37$	$0.906 \pm 0.006 \pm 0.013$	$0.256 \pm 0.002 \pm 0.010$
3. $1.52 < \eta < 2.37$	$0.933 \pm 0.007 \pm 0.009$	$0.431 \pm 0.002 \pm 0.013$

likelihood-based version of a standard matrix method (here called the “likelihood matrix method”). In standard matrix methods [33], a matrix of efficiencies relates an observed event that falls into a particular event category (based on some discriminating variable or variables) to the true, unknown final states to which the event has the possibility of corresponding, and the matrix is inverted to determine probabilities that a given observed event corresponds to one of these true final states. When summed over a large number of events, these per-event estimators average to the overall estimate of the number of events in each true final state.

In the likelihood matrix method, by contrast (and with respect to the present three-photon search), the expected yield for each three-object final state consisting of jets plus photons or all jets is the result of fitting a likelihood function to data. For the event sample where all three photons, ordered from highest to lowest p_T , have satisfied the *tight* requirements, events are placed into 160 orthogonal categories designated by six criteria. These are defined first by the three regions in the p_T - η plane to which each photon candidate belongs. These are the same three regions that are used to categorise photons and to calculate ϵ_γ and f_{jet} , described and labeled previously as regions 1–3. The remaining three criteria by which each event is categorized are three boolean variables, one for each photon candidate, indicating whether it passed or failed the isolation criterion. Since each of the three photon candidates either passes (P) or fails (F) isolation, there are $2^3 = 8$ possible isolation combinations for three photons: PPP, PPF, PFP, FPP, PFF, FPF, FFP, and FFF. The three photons are ordered by p_T , from highest to lowest, and, since one of the three kinematic regions defined above depends only upon η , there are twenty possible p_T - η bin combinations: 333, 332, 323, 322, 331, 313, 311, 321, 222, 223, 232, 233, 221, 211, 231, 213, 111, 113, 131, 133. This results in $8 \times 20 = 160$ categories, denoted PPP_333 for those events where the three photon candidates all passed isolation and had p_T - η values placing them in the “3” kinematic region, PPF_321 for those events where the leading and subleading photons passed isolation and the sub-subleading photon failed isolation, and the p_T - η value combinations placed them successively in the “3”, “2”, and “1” regions, etc.

Each of the 160 categories corresponds to a Poisson function where the observed number of events is the number of events seen in data for that category and the expected number of events is a sum of terms corresponding to each of the possible true (unknown) final states consisting of photons and jets or only jets for a particular p_T - η combination. Each term in a given sum is multiplied by the appropriate values of ϵ_γ and f_{jet} . A likelihood is then constructed consisting of a product of the 160 Poisson functions. The expectations for each true final state are the maximum likelihood estimators that result from fitting this likelihood function to the data. That is, the true unknown expectations are allowed to float in the fit and are constrained to be positive and, hence, physical. The estimated number of events of a given final state in a particular signal or control region – defined by whether the photons passed or failed isolation – is determined by summing the resulting expectations from the fit times the appropriate ϵ_γ and f_{jet} values.

6 Systematic uncertainties

6.1 Data-driven uncertainties

For the data-driven jet background estimate, systematic uncertainties arise in the calculation of the rate of photons passing the isolation criterion, ϵ_γ , and the rate of jets misidentified as isolated photons (“jet fakes”), f_{jet} . This calculation relies upon the assumptions that both the tail ($E_T^{\text{iso}} > 7 \text{ GeV}$) of the E_T^{iso} distribution of *tight* photons and the entirety of the E_T^{iso} distribution of *non-tight* photons are primarily composed of jet fakes. Tests on simulations of photons and jets indicate that the true photon contamination in these jet-dominated regions is between 5 and 15 %, depending on the region. These values are used to calculate different values of ϵ_γ and f_{jet} (where the number of photon candidates in a given region is altered by the corresponding percentage) which are then used in the jet background estimate. The deviations from the nominal signal region yield (assuming no true photon contamination) are calculated separately for the three final states of $2\gamma + 1 \text{ jet}$, $1\gamma + 2 \text{ jets}$, and 3 jets , and

these values (4, 10 and 21 %, respectively) are taken as systematic uncertainties on the estimates of these backgrounds in the signal region.

An additional uncertainty associated with the data-driven methods employed arises from the choice of kinematic variable used to categorise photons and then to calculate and apply ϵ_γ and f_{jet} . The baseline analysis uses three bins in the p_T - η plane, described in Sect. 5, and separate analyses using either p_T -dependence only or η -dependence only are conducted as well. The largest deviation of the two different methods from the nominal method is 13 %, which is taken as a systematic uncertainty.

6.2 Simulation uncertainties

The uncertainty on the integrated luminosity for the data sample is 2.8 %, derived using the same methodology as that detailed in Ref. [34].

The photon identification efficiency has been directly measured in data using photons from $Z \rightarrow e^+e^-/\mu^+\mu^-$ radiative decays [12]. The systematic uncertainties on the signal region yield due to the uncertainty on this efficiency measurement are found to range from <1 to 6 % for simulated backgrounds, and from 3 to 7 % for simulated signal processes, depending on the sample.

As mentioned in Sect. 3, the analysis supplements the isolation prescription – $E_T^{\text{iso}} < 4$ GeV, with a cone size of $\Delta R < 0.4$ – with an isolation energy correction that is applied to photons with overlapping isolation cones. This procedure improves sensitivity to lower-mass two-photon resonances where the photon pairs are close together in ΔR . To account for possible over- or under-correction due to a photon being near the edge of the isolation annulus, an additional systematic uncertainty is assessed. The p_T values of all isolated photons in simulated samples are calibrated to yield agreement with the values observed in data [35]. Since the calibration factors for isolated photons deviate from one by typically less than 5 %, a value of 5 % is a conservative estimate of the uncertainty on photon p_T . To assess the systematic uncertainty on the isolation energy correction, the measured value of the p_T of the other *tight* photon in the isolation cone is varied by 5 %, the correction procedure is applied, and the effects are propagated to the final event selection in the signal region. For example, using simulated samples of a Higgs boson decaying to four photons via $H \rightarrow aa \rightarrow 4\gamma$, the systematic uncertainty due to this effect is smaller for higher ratios of m_a/m_H (as large as 6 % when the p_T is varied by -5 and <1 % when the p_T is varied by $+5$ %, for $m_H = 900$ GeV and $m_a = 440$ GeV), and the uncertainty is larger for smaller ratios of m_a/m_H (as large as 69 % when the p_T is varied by -5 and 12 % when the p_T is varied by $+5$ %, for $m_H = 900$ GeV and $m_a = 50$ GeV), as

the photons tend to overlap within the isolation cone more frequently.

The uncertainties on the event yields due to systematic uncertainties in the photon energy scale and resolution [35] are found to range from <1 to 4 % for the simulated signal and background samples. The uncertainties on the event yields due to systematic uncertainties in the scale factors used to yield agreement between photon identification efficiencies calculated in data and simulated samples [35] are found to range from <1 to 8 % for simulated backgrounds, and from 1 to 4 % for simulated signal processes. The systematic uncertainty on the scaling factor for electrons misidentified as photons in simulated samples is taken to be the statistical uncertainty arising from the calculation, i.e., 4 %, since this is as large as or larger than the systematic uncertainties due to the photon energy scale and resolution, above. The efficiency and uncertainties of the three-photon trigger chain have been determined to be 98.5 ± 0.1 (stat.) ± 0.2 % (syst.). The trigger efficiency is calculated using single photons (with p_T values corresponding to the values used for the analysis event selection) from Z boson radiative decays and then, under the assumption that the per-event performance of the photon trigger for one photon is uncorrelated to that for another photon in the same event, multiplying these values to obtain the overall trigger efficiency.

Uncertainties on calculated cross sections for simulated background processes due to QCD renormalisation and factorisation scales and due to the choice of PDF set and value of α_s used in simulation are addressed via the recommendations of PDF4LHC [36]. The resulting combined uncertainties are found to range from 7 to 16 %, depending on the simulated background process. The total theoretical uncertainty on the SM 3γ background process due to the uncertainty on the LO to NLO correction, combined with the uncertainties due to choice of PDF set and renormalisation and factorisation scales, is found to be ~ 30 %.

Uncertainties exist for the measured or calculated production cross sections for SM particles for which BSM decays are considered as signal scenarios and are accounted for. For the BSM Higgs boson scenario of $h \rightarrow aa \rightarrow 4\gamma$ the gluon fusion production cross section for the SM Higgs boson with $m_h = 125$ GeV [37, 38], $\sigma_{h,\text{SM}} = 19.27$ pb is used, with an uncertainty of ± 10.4 % due to choice of PDF set and renormalisation and factorisation scales. For the rare decay $Z \rightarrow 3\gamma$, the measured $pp \rightarrow Z$ cross section of $(2.79 \pm 0.02 \pm 0.11) \times 10^4$ pb [39] is used. An additional uncertainty of ± 12.3 % – determined by varying the QCD renormalisation and factorisation scales, PDF set, and value of α_s – is also assessed, to account for variations in the simulation of the kinematics of the final-state photons and, hence, the acceptance in the signal region.

These systematic uncertainties are summarized in Table 2.

Table 2 Systematic uncertainties (%) on the expected event yields in the signal region. The values given for data-driven backgrounds correspond to the three jet backgrounds described in the text. For simulated samples, when a range is given it corresponds to the smallest and largest uncertainties for all simulated backgrounds or signals

Data-driven	Background	Signal
Photon contamination of control regions	4–21	–
Kinematic parametrization	13	–
Simulation		
Photon ID	1–6	3–7
Photon isolation correction	<1–4	<1–69
Photon energy scale and resolution	<1–4	<1–4
Photon scale factors	<1–8	1–4
Electron scale factors	4	4
Trigger	0.2	0.2
Luminosity	2.8	2.8
Cross section	7–16	4–12

7 Results and interpretations

This section presents results based on the number of events in a broad inclusive region and a restricted region focusing on the rare decay $Z \rightarrow 3\gamma$, as well as results from the search for resonances in the di-photon and tri-photon invariant mass spectra.

7.1 Inclusive and $Z \rightarrow 3\gamma$ regions

The number of SM background events expected in the signal region is 1370 ± 140 (combined statistical and systematic uncertainties) and the observed number of events is 1290. The observation is in agreement with the SM expectation. Additionally, while the event selection is optimised for a search for physics beyond the SM as opposed to a measurement of the 3γ inclusive cross section, the results are nevertheless compatible with the irreducible all-photon process expectations from the SM. The expected and observed yields in the signal region are presented in Table 3, and the expected and observed yields in signal and control regions where all three photons have passed the *tight* identification criterion are shown in Fig. 2. In the figure, the red hatched band, in the signal region bin, is the combination of statistical and systematic uncertainties on all background sources, while the black hatched band, in the control regions, is the combination of statistical uncertainties of the data-driven jet background estimate and the expected yields from simulated samples of SM background processes. For the inclusive signal region, this corresponds to a model-independent observed (expected $\pm 1\sigma$) upper limit, at the 95 % confidence level (CL), on the number of signal events of 240 (273_{-66}^{+83}), and

Table 3 Expected and observed event yields in the inclusive signal region and for the signal region with a further requirement of $80 \text{ GeV} < m_{3\gamma} < 100 \text{ GeV}$. Background expectations estimated via simulations are marked sim., whereas data-driven calculations are denoted as D–D. The uncertainties for each row are the combination of statistical and systematic uncertainties for a given background process, and the overall uncertainties in the second to last row are the combined uncertainties for the total background expectations for each signal region

Process	Inclusive signal region	$80 \text{ GeV} < m_{3\gamma} < 100 \text{ GeV}$
2γ (sim.)	330 ± 50	24 ± 8
3γ (sim.)	340 ± 110	30 ± 10
4γ (sim.)	1.3 ± 0.4	0.07 ± 0.02
$2\gamma, 1j$ (D–D)	350 ± 60	65 ± 19
$1\gamma, 2j$ (D–D)	110 ± 40	13 ± 10
$3j$ (D–D)	43 ± 11	6.1 ± 2.0
$Z \rightarrow e^+e^-$ (sim.)	85 ± 22	43 ± 13
$Z+\gamma$ (sim.)	89 ± 11	48 ± 6
$W+\gamma+(0,1,2)j$ (sim.)	11.4 ± 1.5	2.7 ± 0.7
$W+2\gamma+(0,1,2)j$ (sim.)	6.1 ± 0.5	0.68 ± 0.08
Total SM exp.	1370 ± 140	233 ± 28
Observed	1290	244

to the model-dependent upper limits on the inclusive fiducial cross section in the aforementioned acceptance for the signal scenarios of the BSM Higgs boson and Higgs boson-like decays and the Z' decays shown in Table 4, where hypothesis testing and limit setting are calculated using the profile likelihood ratio as the test statistic for the CL_s technique [40] in the asymptotic approximation [41, 42]. The fiducial efficiencies for each signal scenario are determined with respect to a generator-level kinematic region with the same requirements applied to three-photon events as those used for the analysis signal region. This fiducial region is defined as the set of events that contain three photons where (1) each photon satisfies a pseudorapidity requirement of $|\eta| < 2.37$, excluding the transition region between the barrel and end-cap of $1.37 < |\eta| < 1.52$, (2) the three photons satisfy $p_T > 22, 22$, and 17 GeV , and (3) each photon satisfies $E_T^{\text{truth iso}} < 4 \text{ GeV}$, where $E_T^{\text{truth iso}}$ is a generator-level definition of the photon isolation criterion equivalent to that used for event selection on reconstructed events. The fiducial efficiencies are similar for the considered signal scenarios for mass points where the distributions of photon p_T , for all photons, tend to peak higher than $p_T > 50 \text{ GeV}$. This is because the overall photon identification efficiency decreases for photons with $p_T < 50 \text{ GeV}$ [12]. Since the p_T distribution for at least one of the photons for signal scenarios with lower-mass resonances tends to peak at lower values, the fiducial efficiencies are lower.

Using the same data-driven and simulation-based methodology restricted to the region $80 \text{ GeV} < m_{3\gamma} < 100 \text{ GeV}$ provides a test for the rare decay of the Z boson to three

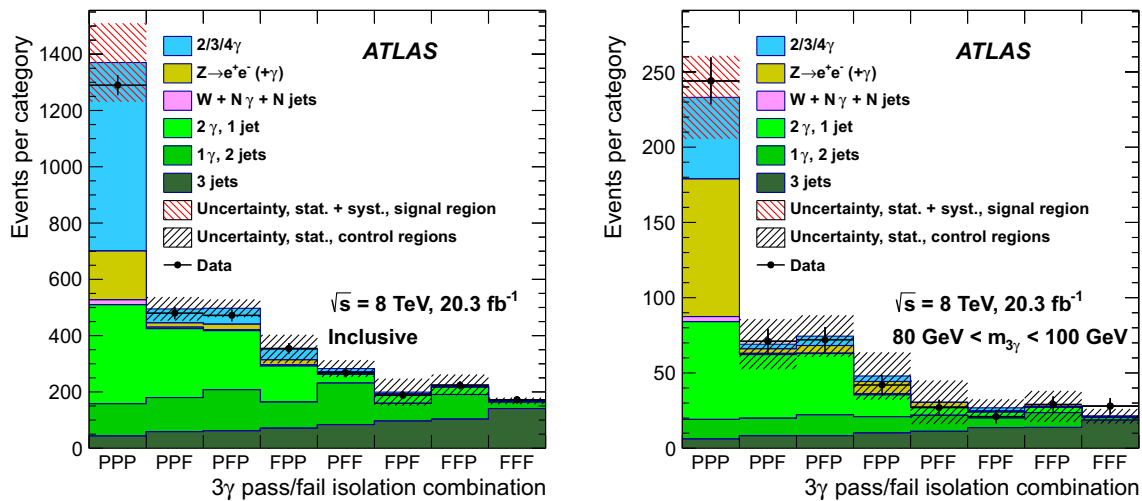


Fig. 2 Observed and expected yields in signal and control regions for the full mass range (*left*) and the restricted range of $80 \text{ GeV} < m_{3\gamma} < 100 \text{ GeV}$ (*right*), for events where all three photon candidates satisfy the *tight* photon identification criteria. The bins along the *horizontal axis* correspond to orthogonal subsets of events where each subset is categorised by whether the three photons – ordered from largest to smallest values of p_T – passed (“P”) or failed (“F”) the isolation criterion. The *leftmost bin* is the signal region, composed of events satisfying PPP, and

the other bins are the different control regions, where at least one of the photon candidates failed the isolation criterion. The *red hatched band*, in the signal region bin, is the combination of statistical and systematic uncertainties, while the *black hatched bands* represent statistical uncertainties. As a result of the data-driven jet background estimate, the statistical uncertainty in each bin is partially correlated with the uncertainty on the data in that bin

Table 4 *Top row* observed and expected model-independent upper limits on event yields for new physics processes for the inclusive signal region. Also shown are the efficiencies for the fiducial kinematic region defined in the text for some example mass points for the signal scenarios explicitly considered here, and the corresponding observed and expected ($\pm 1\sigma$) upper limits on the fiducial cross section within the acceptance. Total statistical uncertainties are quoted for the fiducial efficiencies, and the uncertainties for the upper limits correspond to the uncertainties arising from the $\pm 1\sigma$ upper limits calculated via hypothesis testing using the combination of statistical and systematic uncertainties

Expected background		Observed	Obs. (exp.) 95 % CL upper limit on N_{sig}	
1370 ± 140		1290	$240 (273^{+83}_{-66})$	
Signal process		Fiducial efficiency	Obs. (exp.) upper limit, $\sigma_{\text{fid}} \times \mathcal{A}$ (fb)	Obs. (exp.) upper limit, σ_{overall} (fb)
$h/H \rightarrow aa \rightarrow 4\gamma$				
$m_{h/H}$ (GeV)	m_a (GeV)			
125	10	0.374 ± 0.005	$32 (36^{+11}_{-9})$	$171 (222^{+50}_{-33})$
125	62	0.490 ± 0.004	$24 (27^{+8}_{-7})$	$118 (155^{+23}_{-15})$
300	100	0.643 ± 0.003	$18 (21^{+6}_{-5})$	$29 (35^{+9}_{-7})$
600	100	0.688 ± 0.003	$17 (20^{+6}_{-5})$	$27 (34^{+7}_{-7})$
900	100	0.680 ± 0.003	$17 (20^{+6}_{-5})$	$27 (33^{+7}_{-6})$
$Z' \rightarrow a + \gamma \rightarrow 3\gamma$				
$m_{Z'}$ (GeV)	m_a (GeV)			
100	40	0.438 ± 0.009	$27 (31^{+9}_{-7})$	$316 (387^{+98}_{-75})$
200	100	0.611 ± 0.005	$19 (22^{+7}_{-5})$	$53 (62^{+20}_{-16})$
400	100	0.649 ± 0.004	$18 (21^{+6}_{-5})$	$51 (63^{+14}_{-11})$
600	100	0.667 ± 0.004	$18 (20^{+6}_{-5})$	$39 (48^{+12}_{-9})$
1000	100	0.636 ± 0.004	$19 (21^{+6}_{-5})$	$38 (46^{+11}_{-9})$

photons. The SM branching ratio for the process is predicted to be $\sim 5 \times 10^{-10}$ [9], but it has yet to be observed. Table 3 (right) and Fig. 2 (right) summarise the observed counts as well as background expectations in this restricted region. The data are consistent with the SM expectation: 244 events are

observed and 233 ± 28 events are expected, while the signal expectation from simulation, for $\text{BR}(Z \rightarrow 3\gamma) = 10^{-5}$ (corresponding to the previous limit from LEP [10]), is 418 ± 9 events. Using the same hypothesis-testing and limit-setting procedure described above, but taking the signal expecta-

tion from the simulated sample described in Sect. 4, the observed (expected) limit, at the 95 % CL, on the branching ratio of the Z boson decay to three photons is found to be $\text{BR}(Z \rightarrow 3\gamma) < 2.2 (2.0) \times 10^{-6}$, a result five times stronger than the previous LEP limit of $< 10^{-5}$.

7.2 The 2γ and 3γ resonance searches

In addition to the tests based on the number of events in the inclusive signal regions, searches are performed for resonances in the two-photon and three-photon invariant mass ($m_{2\gamma}$ and $m_{3\gamma}$) distributions for events in the inclusive signal region. For these resonance searches, the background contribution is estimated from a fit to the $m_{2\gamma}$ or $m_{3\gamma}$ sideband regions, and thus does not rely upon simulated samples for the background estimate. The sideband is modelled as a fourth-order polynomial, and the size of the sideband is mass-dependent, symmetric around the hypothesised resonance mass, following a local-spectrum approach. The range of the observed mass spectrum that is used for the sideband fit is a local, truncated subset of the full spectrum. For the $m_{2\gamma}$ ($m_{3\gamma}$) resonance search, the sideband is 20 (25) GeV in each direction for $m_{2\gamma}$ ($m_{3\gamma}$) < 90 (230) GeV, where the event counts change rapidly as a function of $m_{2\gamma}$ ($m_{3\gamma}$), and rises to a sideband size of 80 (100) GeV in each direction for $m_{2\gamma}$ ($m_{3\gamma}$) > 195 (425) GeV, increasing roughly linearly with mass as the spectrum becomes smoother. The $m_{2\gamma}$ ($m_{3\gamma}$) resonance search begins at a mass hypothesis of 10 (100) GeV, and proceeds in steps of 0.5 GeV. The signal component of the resonance search is a Gaussian function with a fixed width that varies with particle mass, and the widths are determined from simulated signal samples. Since the simulated signal samples are generated with a narrow-width approximation for both the pseudoscalar a and the Z' in all cases, the 2γ and 3γ mass resolutions for this search are equivalent to Gaussian functions that account for detector resolution, and are determined via fits to the simulated signal samples. Hypothesis testing and limit setting are performed using the profile likelihood ratio as the test statistic for the CL_s technique in the asymptotic approximation.

The resonance search is performed separately for the three two-photon mass spectra defined by the three possible photon pairings for three photons in the inclusive signal region. As mentioned previously, the photons are ordered by p_T , from highest to lowest, and so the three two-photon mass spectra are denoted m_{12} , m_{13} and m_{23} , where the 1, 2, and 3 refer to the p_T -ordered photons. The observed $m_{2\gamma}$ and $m_{3\gamma}$ spectra in the inclusive signal region are shown in Fig. 3. Also shown in Fig. 3, for visualisation purposes only, is the background expectation per bin, determined from the sideband fit to data as a part of the resonance search. The resonance search is performed with a step size of 0.5 GeV and

so the final results shown in Figs. 4 and 5 demonstrate sensitivity to resonances with widths appropriate to the BSM models considered here. The widths of the bins in Fig. 3 do not correspond to the mass resolution for the signal scenarios in question. The background estimates and significances shown in Fig. 3 provide a complementary comparison of the local agreement between data and expectation. The lower panels show the significance, in units of standard deviations of a Gaussian function, of the observation in each bin, taking into account the fractional uncertainty on the background as a result of the sideband fit. The significances shown in the lower panels in Fig. 3 are derived from the p value for the background-only hypothesis for each bin, calculated using a frequentist binomial parameter test [43–45]. For regions beyond the sensitivity of the search, no background estimate is shown.

For the $H/h \rightarrow aa \rightarrow 4\gamma$ BSM signal scenario, the photon pairing (among the three p_T -ordered photons) that most often corresponds to the photons arising from the decay of the same a particle is (2, 3). As a result, the resonance search in the m_{23} spectrum provides the best sensitivity to this model. The widths of the Gaussian signal component – corresponding to the detector resolution – are taken from simulated samples of a Higgs boson decaying to four photons via a pair of intermediate pseudoscalar a particles, and vary from $0.6 \text{ GeV} < \sigma_{\text{Gauss}} < 3.2 \text{ GeV}$ for $10 \text{ GeV} < m_a < 440 \text{ GeV}$, and are largely independent of $m_{h/H}$.

No excess above background is detected, and upper limits, for a SM-like Higgs boson of $m_h = 125 \text{ GeV}$ (and assuming kinematics associated only with gluon fusion SM Higgs boson production), are calculated. Additionally, limits are set for Higgs boson-like scalars with masses larger than 125 GeV. The results of these resonance searches are shown in Fig. 4 for the SM-like Higgs boson of $m_h = 125 \text{ GeV}$ (in the top row) and, as an example of a higher scalar mass, for $m_H = 600 \text{ GeV}$ (in the bottom row). The resonance search limits for higher values of m_H are limited by the small number of events in the mass spectra at higher values of $m_{2\gamma}$. As shown in Fig. 4, the limits vary as a function of two-photon invariant mass, but an overall upper bound on the limits is determined to be $\sigma \times \text{BR}(h \rightarrow aa) \times \text{BR}(a \rightarrow \gamma\gamma)^2 < 1 \times 10^{-3} \sigma_{\text{SM}}$, for $10 \text{ GeV} < m_a < 62 \text{ GeV}$ for the SM-like Higgs boson of $m_h = 125 \text{ GeV}$ and, for the higher scalar mass case, $\sigma_H \times \text{BR}(H \rightarrow aa) \times \text{BR}(a \rightarrow \gamma\gamma)^2 < 0.02 \text{ pb}$ for lower m_a values in the range $10 \text{ GeV} < m_a < 90 \text{ GeV}$ and $< 0.001 \text{ pb}$ for higher m_a (up to 245 GeV for the resonance search in the m_{23} spectrum for $m_H = 600 \text{ GeV}$ shown in Fig. 4). Additionally, using the expected signal yields from simulated samples, inclusive limits are calculated for $300 \text{ GeV} < m_H < 900 \text{ GeV}$ and for a range of $m_a < m_{H/2}$, including values beyond the range of the mass spectra used for the resonance search. These inclusive limits are shown in Table 5.

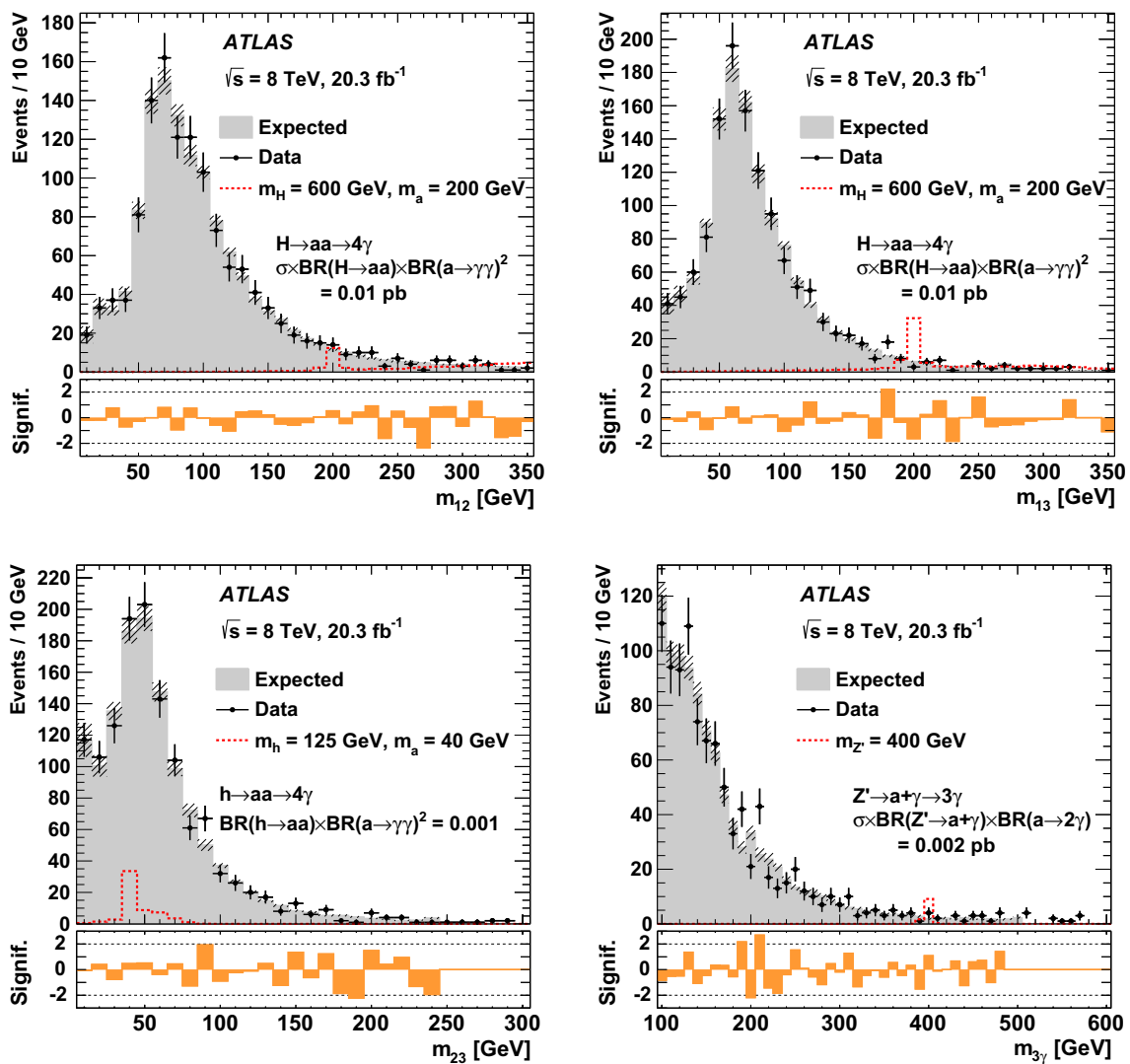


Fig. 3 Observed spectra of m_{12} , m_{13} , and m_{23} , where the 1, 2, and 3 refer to three p_T -ordered photons, as well as $m_{3\gamma}$. For illustration purposes only, also shown is the expected background per bin, determined via unbinned sideband fits to the data as a part of the resonance search, for a hypothesised resonance mass defined by the centre of the bin, as well as the signal expectation for a few mass points for the BSM scenarios considered here. The *lower panels* show the significance, in units of standard deviations of a Gaussian function, of the observation in each bin, taking into account the fractional uncertainty on the background

Moreover, upper limits on the Z' production cross section times the product of branching ratios, $\sigma_{Z'} \times \text{BR}(Z' \rightarrow a + \gamma) \times \text{BR}(a \rightarrow \gamma\gamma)$, are found to be in the range of 0.04 pb to 0.3 pb, depending upon $m_{Z'}$ and m_a . Upper limits, at the 95 % CL, on $\sigma_{Z'} \times \text{BR}(Z' \rightarrow a + \gamma) \times \text{BR}(a \rightarrow \gamma\gamma)$ are shown in Table 6, as a function of m_a , using the expected signal yields from simulated samples. Additionally, using a narrow-width approximation to the Z' resonance width, local excesses corresponding to Gaussian resonances due to detector resolution are searched for in the $m_{3\gamma}$ spectrum. The

as a result of the sideband fit. This significance is derived from the p value for the background-only hypothesis for each bin, calculated using a frequentist binomial parameter test [43–45]. The signal distributions used for the $m_{2\gamma}$ resonance searches have two components, a narrow Gaussian core for correctly paired two-photon combinations and a wide distribution for incorrectly paired combinations that is well described by the polynomial used to simultaneously model the background shape for the resonance search described in Sect. 7.2

Gaussian widths are determined via fits to the Z' simulated signal samples, described in Sect. 4. For the range of $m_{Z'}$ for which the resonance search is possible, the Z' width exhibits a small dependence on m_a . For each Z' mass point, three different samples are simulated, with different values of m_a . The average of the three measured Z' widths for each of the m_a points simulated is taken as the width for a given $m_{Z'}$, and these values are used for the three-photon resonance search, interpolating for $m_{Z'}$ points between those for which samples are simulated. These values range from $1.5 \text{ GeV} < \sigma_{\text{Gauss}} <$

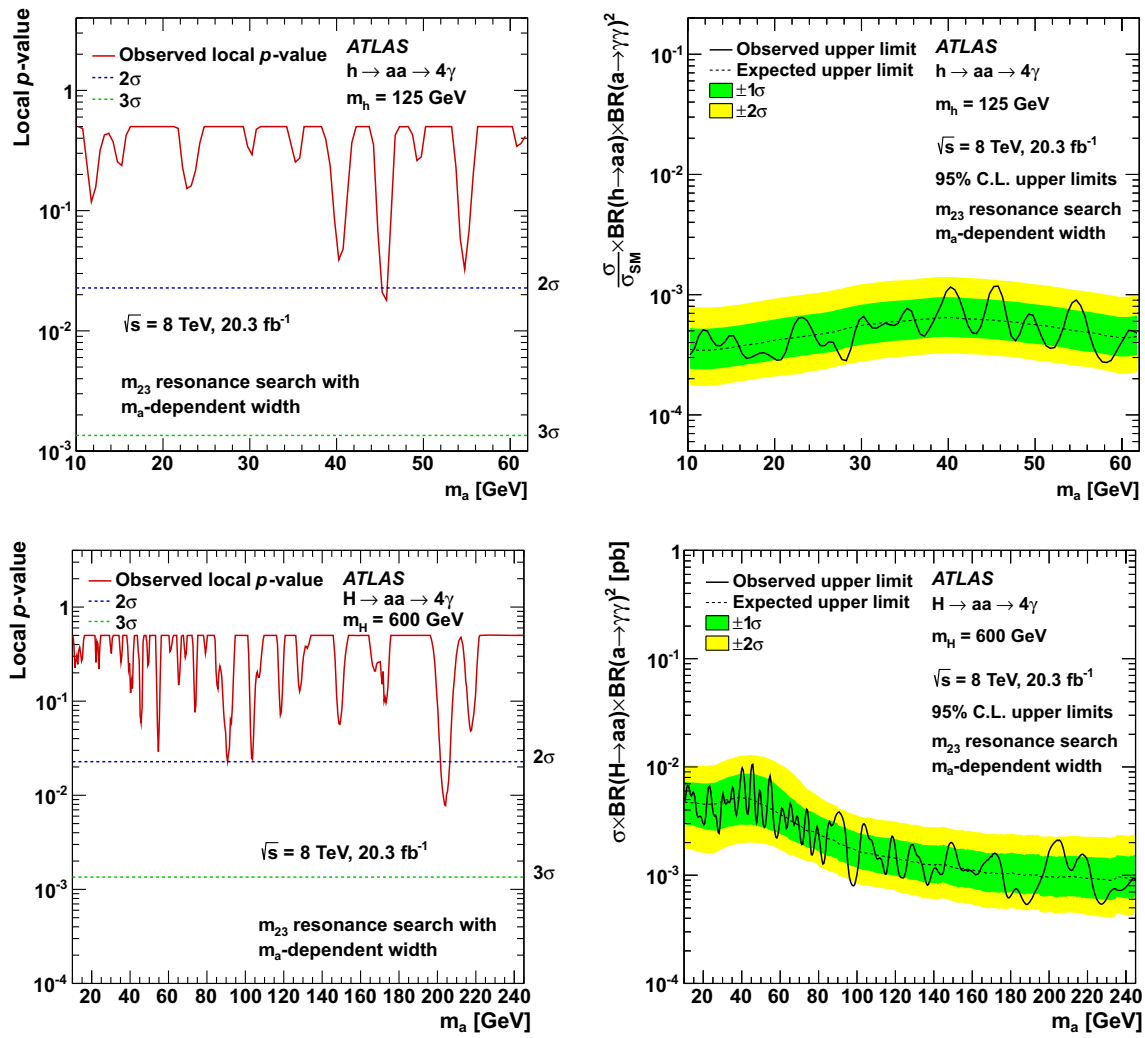


Fig. 4 Left local p values for the background-only hypothesis as a result of a resonance search with respect to the BSM process $h/H \rightarrow aa \rightarrow 4\gamma$, for $m_h = 125$ GeV (top row) and $m_H = 600$ GeV (bottom row), as a function of m_a , determined via a search for local excesses in the m_{23} spectrum. Right upper limits, at the 95 % CL, on $(\sigma/\sigma_{SM}) \times BR(h \rightarrow aa) \times BR(a \rightarrow \gamma\gamma)^2$ (top row) and

$\sigma_H \times BR(H \rightarrow aa) \times BR(a \rightarrow \gamma\gamma)^2$ (bottom row). Also shown are the ± 1 and 2σ uncertainty bands resulting from the resonance search hypothesis tests, taking into account the statistical and systematic uncertainties from simulated signal samples which are used to determine signal efficiency and Gaussian resonance width due to detector resolution for each mass hypothesis

Table 5 Expected and observed 95 % CL upper limits on $\sigma_H \times BR(H \rightarrow aa) \times BR(a \rightarrow \gamma\gamma)^2$. The uncertainties for the expected limits are the $\pm 1\sigma$ uncertainties resulting from the hypothesis tests for each mass point, taking into account statistical and systematic uncertainties

m_H (GeV)	m_a (GeV)			
	$\sigma_H \times BR(H \rightarrow aa) \times BR(a \rightarrow \gamma\gamma)^2$ (fb)			
	20	50	100	140
300	48 (60^{+13}_{-10})	33 (40^{+9}_{-8})	29 (35^{+9}_{-7})	28 (34^{+8}_{-6})
	50	100	200	290
600	31 (38^{+10}_{-7})	27 (34^{+7}_{-7})	25 (31^{+7}_{-6})	25 (31^{+7}_{-6})
	50	100	200	440
900	36 (44^{+11}_{-8})	27 (33^{+7}_{-6})	26 (33^{+7}_{-6})	26 (32^{+7}_{-5})

2.4 GeV for $100 \text{ GeV} < m_{Z'} < 500 \text{ GeV}$. The results, along with the local p values for the background-only hypothesis, are shown in Fig. 5. The smallest local p value is found to be 0.0003 (3.4σ local significance), at $m_{3\gamma} = 212 \text{ GeV}$ which, after adjusting for a trials factor [46], corresponds to a global p value of 0.087 (1.4σ global significance).

8 Conclusion

A search for new phenomena in events with at least three photons has been performed using 20.3 fb^{-1} of LHC pp collision data at $\sqrt{s} = 8 \text{ TeV}$ collected with the ATLAS detector at CERN. The SM background expectation is in agreement with

Table 6 Expected and observed 95 % CL upper limits on $\sigma_{Z'} \times \text{BR}(Z' \rightarrow a + \gamma) \times \text{BR}(a \rightarrow \gamma\gamma)$. The uncertainties for the expected limits are the $\pm 1\sigma$ uncertainties resulting from the hypothesis tests for each mass point, taking into account statistical and systematic uncertainties

$m_{Z'}$ (GeV)	m_a (GeV)		
	$\sigma_{Z'} \times \text{BR}(Z' \rightarrow a + \gamma) \times \text{BR}(a \rightarrow \gamma\gamma)$ (fb)		
Observed (expected) 95 % CL upper limits			
	40	60	80
100	320 (390^{+98}_{-70})	150 (170^{+50}_{-40})	310 (370^{+100}_{-80})
	50	100	150
200	78 (90^{+28}_{-22})	53 (62^{+20}_{-16})	51 (58^{+19}_{-14})
	100	200	300
400	51 (63^{+14}_{-10})	44 (55^{+12}_{-9})	38 (47^{+12}_{-10})
	100	250	400
600	39 (48^{+12}_{-9})	41 (52^{+10}_{-8})	41 (52^{+11}_{-8})
	100	350	600
800	38 (46^{+11}_{-9})	35 (43^{+9}_{-8})	35 (43^{+9}_{-9})
	100	450	800
1000	38 (46^{+11}_{-9})	54 (64^{+17}_{-10})	37 (43^{+12}_{-8})

the data, and is determined to be 1370 ± 140 events while 1290 events are observed. The model-independent observed (expected) 95 % CL upper limit on the number of signal events is found to be 240 (273^{+83}_{-66}). Upper limits at the 95 % CL are calculated on the fiducial cross section σ_{fid} for events from non-SM processes for several signal scenarios. The observed (expected) limit on the branching ratio of the Z

boson decay to three photons is found to be $\text{BR}(Z \rightarrow 3\gamma) < 2.2 (2.0) \times 10^{-6}$, a result five times stronger than the previous result from LEP.

In addition, a search for local excesses in the two-photon and three-photon invariant mass distributions is conducted. For the two-photon mass spectra, no significant excesses are detected, and the 95 % CL upper limit on $(\sigma/\sigma_{\text{SM}}) \times \text{BR}(h \rightarrow aa) \times \text{BR}(a \rightarrow \gamma\gamma)^2$ (assuming kinematics associated only with gluon fusion SM Higgs boson production) is calculated to vary from $\sim 3 \times 10^{-4}$ to $\sim 4 \times 10^{-4}$ for $10 \text{ GeV} < m_a < 62 \text{ GeV}$ for a SM-like Higgs boson with a mass of $m_h = 125 \text{ GeV}$. Limits are set for Higgs boson-like scalars H with masses up to $m_H = 900 \text{ GeV}$ and are found to be $\sigma_H \times \text{BR}(H \rightarrow aa) \times \text{BR}(a \rightarrow \gamma\gamma)^2 < 0.02\text{--}0.001 \text{ pb}$, depending upon m_H and m_a . For the three-photon mass spectrum, the resonance search is conducted in the context of a Z' decaying to three photons. The smallest local p value is found to be 0.0003 (3.4σ local significance), at $m_{Z'} = 212 \text{ GeV}$ which, after adjusting for a trials factor, corresponds to a global p value of 0.09 (1.4σ global significance). Upper limits at the 95 % CL on the Z' production cross section times the product of branching ratios, $\sigma_{Z'} \times \text{BR}(Z' \rightarrow a + \gamma) \times \text{BR}(a \rightarrow \gamma\gamma)$, are found to be in the range of 0.04–0.3 pb, depending upon $m_{Z'}$.

These model-independent results are the first of their kind, as are the interpretations for a Higgs boson decaying to four photons via two intermediate pseudoscalar a particles (for a SM-like Higgs boson of $m_h = 125 \text{ GeV}$ and for Higgs-like scalars of higher masses) and for three-photon resonances corresponding to a new vector gauge boson.

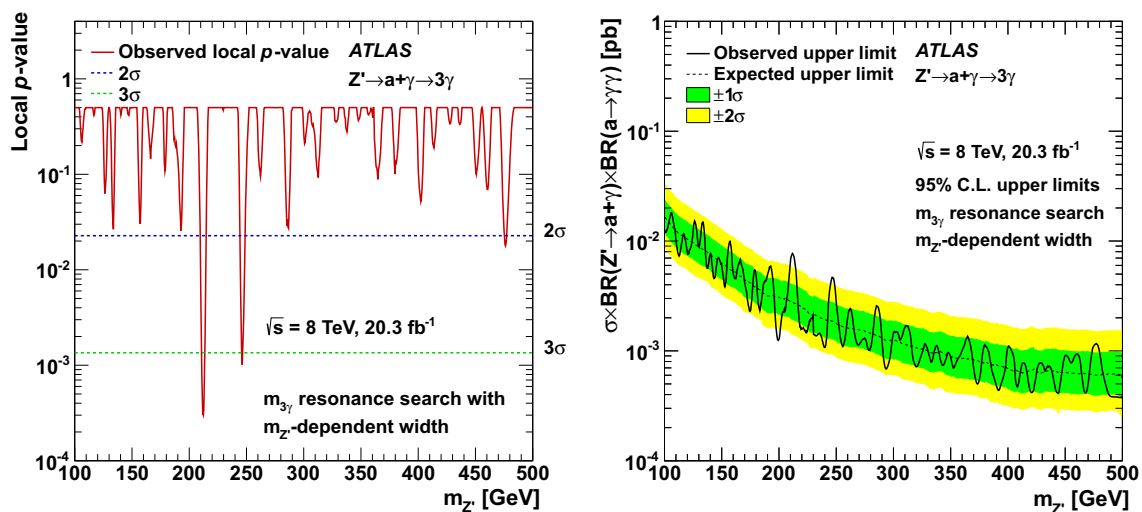


Fig. 5 Left local p values for the background-only hypothesis as a result of a resonance search with respect to the production of a new vector gauge boson Z' as a function of $m_{Z'}$, determined via a search for local excesses in the $m_{3\gamma}$ spectrum, using a narrow-width approximation to the Z' resonance width. The smallest local p value is found to be 0.0003 (3.4σ) which corresponds to a global p value of 0.087 (1.4σ). Right

upper limits, at the 95 % CL, on $\sigma_{Z'} \times \text{BR}(Z' \rightarrow a + \gamma) \times \text{BR}(a \rightarrow \gamma\gamma)$. Also shown are the ± 1 and 2σ uncertainty bands resulting from the resonance search hypothesis tests, taking into account the statistical and systematic uncertainties from simulated signal samples which are used to determine signal efficiency and Gaussian resonance width due to detector resolution for each mass hypothesis

Acknowledgments We thank CERN for the very successful operation of the LHC, as well as the support staff from our institutions without whom ATLAS could not be operated efficiently. We acknowledge the support of ANPCyT, Argentina; YerPhI, Armenia; ARC, Australia; BMWFW and FWF, Austria; ANAS, Azerbaijan; SSTC, Belarus; CNPq and FAPESP, Brazil; NSERC, NRC and CFI, Canada; CERN; CONICYT, Chile; CAS, MOST and NSFC, China; COLCIENCIAS, Colombia; MSMT CR, MPO CR and VSC CR, Czech Republic; DNRF, DNSRC and Lundbeck Foundation, Denmark; EPLANET, ERC and NSRF, European Union; IN2P3-CNRS, CEA-DSM/IRFU, France; GNSF, Georgia; BMBF, DFG, HGF, MPG and AvH Foundation, Germany; GSRT and NSRF, Greece; RGC, Hong Kong SAR, China; ISF, MINERVA, GIF, I-CORE and Benoziyo Center, Israel; INFN, Italy; MEXT and JSPS, Japan; CNRST, Morocco; FOM and NWO, Netherlands; BRF and RCN, Norway; MNiSW and NCN, Poland; GRICES and FCT, Portugal; MNE/IFA, Romania; MES of Russia and NRC KI, Russian Federation; JINR; MSTD, Serbia; MSSR, Slovakia; ARRS and MIZŠ, Slovenia; DST/NRF, South Africa; MINECO, Spain; SRC and Wallenberg Foundation, Sweden; SER, SNSF and Cantons of Bern and Geneva, Switzerland; NSC, Taiwan; TAEK, Turkey; STFC, the Royal Society and Leverhulme Trust, United Kingdom; DOE and NSF, United States of America. The crucial computing support from all WLCG partners is acknowledged gratefully, in particular from CERN and the ATLAS Tier-1 facilities at TRIUMF (Canada), NDGF (Denmark, Norway, Sweden), CC-IN2P3 (France), KIT/GridKA (Germany), INFN-CNAF (Italy), NL-T1 (Netherlands), PIC (Spain), ASGC (Taiwan), RAL (UK) and BNL (USA) and in the Tier-2 facilities worldwide.

Open Access This article is distributed under the terms of the Creative Commons Attribution 4.0 International License (<http://creativecommons.org/licenses/by/4.0/>), which permits unrestricted use, distribution, and reproduction in any medium, provided you give appropriate credit to the original author(s) and the source, provide a link to the Creative Commons license, and indicate if changes were made. Funded by SCOAP³.

References

1. S. Chang, P.J. Fox, N. Weiner, Visible cascade Higgs decays to four photons at hadron colliders. *Phys. Rev. Lett.* **98**, 111802 (2007). [arXiv:hep-ph/0608310](https://arxiv.org/abs/hep-ph/0608310)
2. B.A. Dobrescu, G.L. Landsberg, K.T. Matchev, Higgs boson decays to CP odd scalars at the Tevatron and beyond. *Phys. Rev. D* **63**, 075003 (2001). [arXiv:hep-ph/0005308](https://arxiv.org/abs/hep-ph/0005308)
3. F. Larios, G. Tavares-Velasco, C. Yuan, Update on a very light CP odd scalar in the two Higgs doublet model. *Phys. Rev. D* **66**, 075006 (2002). [arXiv:hep-ph/0205204](https://arxiv.org/abs/hep-ph/0205204)
4. D. Curtin et al., Exotic decays of the 125 GeV Higgs boson. *Phys. Rev. D* **90**, 075004 (2014). [arXiv:1312.4992](https://arxiv.org/abs/1312.4992) [hep-ph]
5. R. Dermisek, J.F. Gunion, The NMSSM solution to the fine-tuning problem, precision electroweak constraints and the largest LEP Higgs event excess. *Phys. Rev. D* **76**, 095006 (2007). [arXiv:0705.4387](https://arxiv.org/abs/hep-ph/0705.4387) [hep-ph]
6. ATLAS Collaboration, Observation of a new particle in the search for the Standard Model Higgs boson with the ATLAS detector at the LHC. *Phys. Lett. B* **716**, 1–29 (2012). [arXiv:1207.7214](https://arxiv.org/abs/1207.7214) [hep-ex]
7. CMS Collaboration, Observation of a new boson at a mass of 125 GeV with the CMS experiment at the LHC. *Phys. Lett. B* **716**, 30–61 (2012). [arXiv:1207.7235](https://arxiv.org/abs/1207.7235) [hep-ex]
8. N. Toro, I. Yavin, Multiphotons and photon jets from new heavy vector bosons. *Phys. Rev. D* **86**, 055005 (2012). [arXiv:1202.6377](https://arxiv.org/abs/1202.6377) [hep-ph]
9. E.N. Glover, A. Morgan, Z boson decay into photons. *Z. Phys. C* **60**, 175–180 (1993)
10. L3 Collaboration, M. Acciarri et al., Search for anomalous $Z \rightarrow \gamma\gamma\gamma$ events at LEP. *Phys. Lett. B* **345**, 609–616 (1995)
11. ATLAS Collaboration, The ATLAS experiment at the CERN Large Hadron Collider. *JINST* **3**, S08003 (2008)
12. ATLAS Collaboration, Measurements of the photon identification efficiency with the ATLAS detector using 4.9 fb^{-1} of pp collision data collected in 2011. ATLAS-CONF-2012-123. <http://cds.cern.ch/record/1473426>. Accessed 13 Apr 2016
13. T. Sjöstrand, S. Mrenna, P.Z. Skands, A. Brief, Introduction to PYTHIA 8.1. *Comput. Phys. Commun.* **178**, 852–867 (2008). [arXiv:0710.3820](https://arxiv.org/abs/hep-ph/0710.3820) [hep-ph]
14. J. Alwall, M. Herquet, F. Maltoni, O. Mattelaer, T. Stelzer, MadGraph 5: going beyond. *JHEP* **1106**, 128 (2011). [arXiv:1106.0522](https://arxiv.org/abs/1106.0522) [hep-ph]
15. J.M. Campbell, C. Williams, Triphoton production at hadron colliders. *Phys. Rev. D* **89**, 113001 (2014). [arXiv:1403.2641](https://arxiv.org/abs/1403.2641) [hep-ph]
16. J. Baglio et al., Release note – VBFNLO 2.7.0. [arXiv:1404.3940](https://arxiv.org/abs/1404.3940) [hep-ph]
17. K. Arnold et al., a parton level Monte Carlo for processes with electroweak bosons – manual for version 2.5.0. [arXiv:1107.4038](https://arxiv.org/abs/1107.4038) [hep-ph]
18. K. Arnold et al., VBFNLO: a parton level Monte Carlo for processes with electroweak bosons. *Comput. Phys. Commun.* **180**, 1661–1670 (2009). [arXiv:0811.4559](https://arxiv.org/abs/0811.4559) [hep-ph]
19. J. Pumplin et al., New generation of parton distributions with uncertainties from global QCD analysis. *JHEP* **0207**, 012 (2002). [arXiv:hep-ph/0201195](https://arxiv.org/abs/hep-ph/0201195)
20. H.-L. Lai et al., New parton distributions for collider physics. *Phys. Rev. D* **82**, 074024 (2010). [arXiv:1007.2241](https://arxiv.org/abs/1007.2241) [hep-ph]
21. A. Martin, W. Stirling, R. Thorne, G. Watt, Parton distributions for the LHC. *Eur. Phys. J. C* **63**, 189–285 (2009). [arXiv:0901.0002](https://arxiv.org/abs/0901.0002) [hep-ph]
22. S. Alioli, P. Nason, C. Oleari, E. Re, NLO Higgs boson production via gluon fusion matched with shower in POWHEG. *JHEP* **0904**, 002 (2009). [arXiv:0812.0578](https://arxiv.org/abs/0812.0578) [hep-ph]
23. T. Gleisberg et al., Event generation with SHERPA 1.1. *JHEP* **0902**, 007 (2009). [arXiv:0811.4622](https://arxiv.org/abs/0811.4622) [hep-ph]
24. M.L. Mangano, M. Moretti, F. Piccinini, R. Pittau, A.D. Polosa, ALPGEN, a generator for hard multiparton processes in hadronic collisions. *JHEP* **0307**, 001 (2003). [arXiv:hep-ph/0206293](https://arxiv.org/abs/hep-ph/0206293)
25. G. Corcella et al., HERWIG 6: an event generator for hadron emission reactions with interfering gluons (including supersymmetric processes). *JHEP* **0101**, 010 (2001). [arXiv:hep-ph/0011363](https://arxiv.org/abs/hep-ph/0011363)
26. G. Corcella et al., HERWIG 6.5 release note. [arXiv:hep-ph/0210213](https://arxiv.org/abs/hep-ph/0210213)
27. A. Alloul, N.D. Christensen, C. Degrande, C. Duhr, B. Fuks, FeynRules 2.0 – a complete toolbox for tree-level phenomenology. [arXiv:1310.1921](https://arxiv.org/abs/1310.1921) [hep-ph]
28. C. Degrande et al., UFO – The Universal FeynRules Output. *Comput. Phys. Commun.* **183**, 1201–1214 (2012). [arXiv:1108.2040](https://arxiv.org/abs/1108.2040) [hep-ph]
29. M. Stöhr, J. Hořejší, Effective lagrangians for the Z boson decay into photons. *Phys. Rev. D* **49**, 3775–3778 (1994)
30. A. Gutierrez-Rodriguez, C. Honorato, J. Montano, M. Pérez, Limits on the quartic couplings $Z\gamma\gamma\gamma$ and $ZZ\gamma\gamma$ from e^+e^- colliders. *Phys. Rev. D* **89**, 034003 (2014). [arXiv:1304.7410](https://arxiv.org/abs/1304.7410) [hep-ph]
31. ATLAS Collaboration, The ATLAS simulation infrastructure. *Eur. Phys. J. C* **70**, 823–874 (2010). [arXiv:1005.4568](https://arxiv.org/abs/1005.4568) [physics.ins-det]
32. GEANT4 Collaboration, S. Agostinelli et al., GEANT4: a simulation toolkit. *Nucl. Instrum. Methods A* **506**, 250–303 (2003)
33. ATLAS Collaboration, Measurement of the isolated di-photon cross-section in pp TeV with the ATLAS detector. *Phys. Rev. D* **85**, 012003 (2012). [arXiv:1107.0581](https://arxiv.org/abs/1107.0581) [hep-ex]
34. ATLAS Collaboration, Improved luminosity determination in pp collisions at $\sqrt{s} = 7$ TeV using the ATLAS detector at the LHC. *Eur. Phys. J. C* **73**, 2518 (2013). [arXiv:1302.4393](https://arxiv.org/abs/1302.4393) [hep-ex]

35. ATLAS Collaboration, Electron and photon energy calibration with the ATLAS detector using LHC Run 1 data. *Eur. Phys. J. C* **74**, 3071 (2014). [arXiv:1407.5063](#) [hep-ex]
36. M. Botje et al., The PDF4LHC working group interim recommendations. [arXiv:1101.0538](#) [hep-ph]
37. LHC Higgs Cross Section Working Group Collaboration, S. Dittmaier et al., Handbook of LHC Higgs cross sections: 1. Inclusive observables. [arXiv:1101.0593](#) [hep-ph]
38. LHC Higgs Cross Section Working Group Collaboration, S. Dittmaier et al., Handbook of LHC Higgs cross sections: 2. Differential distributions. [arXiv:1201.3084](#) [hep-ph]
39. ATLAS Collaboration, Measurement of the inclusive W^\pm TeV with the ATLAS detector. *Phys. Rev. D* **85**, 072004 (2012). [arXiv:1109.5141](#) [hep-ex]
40. A.L. Read, Presentation of search results: the CL_s technique. *J. Phys. G Nucl. Part. Phys.* **28**, 2693 (2002)
41. G. Cowan, K. Cranmer, E. Gross, O. Vitells, Asymptotic formulae for likelihood-based tests of new physics. *Eur. Phys. J. C* **71**, 1554 (2011). [arXiv:1007.1727](#) [physics.data-an]
42. G. Cowan, K. Cranmer, E. Gross, O. Vitells, Erratum to: asymptotic formulae for likelihood-based tests of new physics. *Eur. Phys. J. C* **73**, 2501 (2013)
43. R.D. Cousins, J.T. Linnemann, J. Tucker, Evaluation of three methods for calculating statistical significance when incorporating a systematic uncertainty into a test of the background-only hypothesis for a Poisson process. *Nucl. Instrum. Methods Phys. Res. A* **595**, 480–501 (2008). [arXiv:physics.data-an/0702156](#)
44. K. Cranmer, Statistical challenges for searches for new physics at the LHC, in *Proceedings of PhyStat05: Statistical Problems in Particle Physics, Astrophysics and Cosmology*, Oxford, 2005–2006, pp. 112–123. [arXiv:physics.data-an/0511028](#)
45. J. Linnemann, Measures of significance in HEP and astrophysics, in *Proceedings of PhyStat03: Statistical Problems in Particle Physics, Astrophysics and Cosmology*, 2003, p. 35. [arXiv:physics.data-an/0312059](#)
46. E. Gross, O. Vitells, Trial factors or the look elsewhere effect in high energy physics. *Eur. Phys. J. C* **70**, 525–530 (2010). [arXiv:1005.1891](#) [physics.data-an]

ATLAS Collaboration

G. Aad⁸⁵, B. Abbott¹¹³, J. Abdallah¹⁵¹, O. Abdinov¹¹, R. Aben¹⁰⁷, M. Abolins⁹⁰, O. S. AbouZeid¹⁵⁸, H. Abramowicz¹⁵³, H. Abreu¹⁵², R. Abreu¹¹⁶, Y. Abulaiti^{146a,146b}, B. S. Acharya^{164a,164b,a}, L. Adamczyk^{38a}, D. L. Adams²⁵, J. Adelman¹⁰⁸, S. Adomeit¹⁰⁰, T. Adye¹³¹, A. A. Affolder⁷⁴, T. Agatonovic-Jovin¹³, J. Agricola⁵⁴, J. A. Aguilar-Saavedra^{126a,126f}, S. P. Ahlen²², F. Ahmadov^{65,b}, G. Aielli^{133a,133b}, H. Akerstedt^{146a,146b}, T. P. A. Åkesson⁸¹, A. V. Akimov⁹⁶, G. L. Alberghi^{20a,20b}, J. Albert¹⁶⁹, S. Albrand⁵⁵, M. J. Alconada Verzini⁷¹, M. Aleksa³⁰, I. N. Aleksandrov⁶⁵, C. Alexa^{26b}, G. Alexander¹⁵³, T. Alexopoulos¹⁰, M. Alhroob¹¹³, G. Alimonti^{91a}, L. Alio⁸⁵, J. Alison³¹, S. P. Alkire³⁵, B. M. M. Allbrooke¹⁴⁹, P. P. Allport⁷⁴, A. Aloisio^{104a,104b}, A. Alonso³⁶, F. Alonso⁷¹, C. Alpigiani⁷⁶, A. Altheimer³⁵, B. Alvarez Gonzalez³⁰, D. Álvarez Piqueras¹⁶⁷, M. G. Alvigi^{104a,104b}, B. T. Amadio¹⁵, K. Amako⁶⁶, Y. Amaral Coutinho^{24a}, C. Amelung²³, D. Amidei⁸⁹, S. P. Amor Dos Santos^{126a,126c}, A. Amorim^{126a,126b}, S. Amoroso⁴⁸, N. Amram¹⁵³, G. Amundsen²³, C. Anastopoulos¹³⁹, L. S. Ancu⁴⁹, N. Andari¹⁰⁸, T. Andeen³⁵, C. F. Anders^{58b}, G. Anders³⁰, J. K. Anders⁷⁴, K. J. Anderson³¹, A. Andreazza^{91a,91b}, V. Andrei^{58a}, S. Angelidakis⁹, I. Angelozzi¹⁰⁷, P. Anger⁴⁴, A. Angerami³⁵, F. Anghinolfi³⁰, A. V. Anisenkov^{109,c}, N. Anjos¹², A. Annovi^{124a,124b}, M. Antonelli⁴⁷, A. Antonov⁹⁸, J. Antos^{144b}, F. Anulli^{132a}, M. Aoki⁶⁶, L. Aperio Bella¹⁸, G. Arabidze⁹⁰, Y. Arai⁶⁶, J. P. Araque^{126a}, A. T. H. Arce⁴⁵, F. A. Arduh⁷¹, J.-F. Arguin⁹⁵, S. Argyropoulos⁶³, M. Arik^{19a}, A. J. Armbruster³⁰, O. Arnaez³⁰, V. Arnal⁸², H. Arnold⁴⁸, M. Arratia²⁸, O. Arslan²¹, A. Artamonov⁹⁷, G. Artoni²³, S. Asai¹⁵⁵, N. Asbah⁴², A. Ashkenazi¹⁵³, B. Åsman^{146a,146b}, L. Asquith¹⁴⁹, K. Assamagan²⁵, R. Astalos^{144a}, M. Atkinson¹⁶⁵, N. B. Atlay¹⁴¹, K. Augsten¹²⁸, M. Aurousseau^{145b}, G. Avolio³⁰, B. Axen¹⁵, M. K. Ayoub¹¹⁷, G. Azuelos^{95,d}, M. A. Baak³⁰, A. E. Baas^{58a}, M. J. Baca¹⁸, C. Bacci^{134a,134b}, H. Bachacou¹³⁶, K. Bachas¹⁵⁴, M. Backes³⁰, M. Backhaus³⁰, P. Bagiacchi^{132a,132b}, P. Bagnaia^{132a,132b}, Y. Bai^{33a}, T. Bain³⁵, J. T. Baines¹³¹, O. K. Baker¹⁷⁶, E. M. Baldwin^{109,c}, P. Balek¹²⁹, T. Balestri¹⁴⁸, F. Balli⁸⁴, W. K. Balunas¹²², E. Banas³⁹, Sw. Banerjee¹⁷³, A. A. E. Bannoura¹⁷⁵, H. S. Bansil¹⁸, L. Barak³⁰, E. L. Barberio⁸⁸, D. Barberis^{50a,50b}, M. Barbero⁸⁵, T. Barillari¹⁰¹, M. Barisonzi^{164a,164b}, T. Barklow¹⁴³, N. Barlow²⁸, S. L. Barnes⁸⁴, B. M. Barnett¹³¹, R. M. Barnett¹⁵, Z. Barnovska⁵, A. Baroncelli^{134a}, G. Barone²³, A. J. Barr¹²⁰, F. Barreiro⁸², J. Barreiro Guimarães da Costa⁵⁷, R. Bartoldus¹⁴³, A. E. Barton⁷², P. Bartos^{144a}, A. Basalae¹²³, A. Bassalat¹¹⁷, A. Basye¹⁶⁵, R. L. Bates⁵³, S. J. Batista¹⁵⁸, J. R. Batley²⁸, M. Battaglia¹³⁷, M. Bauce^{132a,132b}, F. Bauer¹³⁶, H. S. Bawa^{143,e}, J. B. Beacham¹¹¹, M. D. Beattie⁷², T. Beau⁸⁰, P. H. Beauchemin¹⁶¹, R. Beccherle^{124a,124b}, P. Bechtel²¹, H. P. Beck^{17,f}, K. Becker¹²⁰, M. Becker⁸³, M. Beckingham¹⁷⁰, C. Becot¹¹⁷, A. J. Beddall^{19b}, A. Beddall^{19b}, V. A. Bednyakov⁶⁵, C. P. Bee¹⁴⁸, L. J. Beemster¹⁰⁷, T. A. Beerman³⁰, M. Begel²⁵, J. K. Behr¹²⁰, C. Belanger-Champagne⁸⁷, W. H. Bell⁴⁹, G. Bella¹⁵³, L. Bellagamba^{20a}, A. Bellerive²⁹, M. Bellomo⁸⁶, K. Belotskiy⁹⁸, O. Beltramello³⁰, O. Benary¹⁵³, D. Bencheikroun^{135a}, M. Bender¹⁰⁰, K. Bendtz^{146a,146b}, N. Benekos¹⁰, Y. Benhammou¹⁵³, E. Benhar Nocchioli⁴⁹, J. A. Benitez Garcia^{159b}, D. P. Benjamin⁴⁵, J. R. Bensinger²³, S. Bentvelsen¹⁰⁷, L. Beresford¹²⁰, M. Beretta⁴⁷, D. Berge¹⁰⁷, E. Bergeaas Kuutmann¹⁶⁶, N. Berger⁵, F. Berghaus¹⁶⁹, J. Beringer¹⁵, C. Bernard²², N. R. Bernard⁸⁶, C. Bernius¹¹⁰, F. U. Bernlochner²¹, T. Berry⁷⁷, P. Berta¹²⁹, C. Bertella⁸³, G. Bertoli^{146a,146b}, F. Bertolucci^{124a,124b}, C. Bertsche¹¹³, D. Bertsche¹¹³, M. I. Besana^{91a}, G. J. Besjes³⁶, O. Bessidskaia Bylund^{146a,146b}, M. Bessner⁴², N. Besson¹³⁶, C. Betancourt⁴⁸, S. Bethke¹⁰¹, A. J. Bevan⁷⁶, W. Bhimji¹⁵,

R. M. Bianchi¹²⁵, L. Bianchini²³, M. Bianco³⁰, O. Biebel¹⁰⁰, D. Biedermann¹⁶, S. P. Bieniek⁷⁸, M. Biglietti^{134a}, J. Bilbao De Mendizabal⁴⁹, H. Bilokon⁴⁷, M. Bindi⁵⁴, S. Binet¹¹⁷, A. Bingul^{19b}, C. Bini^{132a,132b}, S. Biondi^{20a,20b}, D. M. Bjerggaard⁴⁵, C. W. Black¹⁵⁰, J. E. Black¹⁴³, K. M. Black²², D. Blackburn¹³⁸, R. E. Blair⁶, J.-B. Blanchard¹³⁶, J. E. Blanco⁷⁷, T. Blazek^{144a}, I. Bloch⁴², C. Blocker²³, W. Blum^{83,*}, U. Blumenschein⁵⁴, G. J. Bobbink¹⁰⁷, V. S. Bobrovnikov^{109,c}, S. S. Bocchetta⁸¹, A. Bocci⁴⁵, C. Bock¹⁰⁰, M. Boehler⁴⁸, J. A. Bogaerts³⁰, D. Bogavac¹³, A. G. Bogdanchikov¹⁰⁹, C. Bohm^{146a}, V. Boisvert⁷⁷, T. Bold^{38a}, V. Boldea^{26b}, A. S. Boldyrev⁹⁹, M. Bomben⁸⁰, M. Bona⁷⁶, M. Boonekamp¹³⁶, A. Borisov¹³⁰, G. Borissov⁷², S. Borroni⁴², J. Bortfeldt¹⁰⁰, V. Bortolotto^{60a,60b,60c}, K. Bos¹⁰⁷, D. Boscherini^{20a}, M. Bosman¹², J. Boudreau¹²⁵, J. Bouffard², E. V. Bouhova-Thacker⁷², D. Boumediene³⁴, C. Bourdarios¹¹⁷, N. Bousson¹¹⁴, S. K. Boutle⁵³, A. Boveia³⁰, J. Boyd³⁰, I. R. Boyko⁶⁵, I. Bozic¹³, J. Bracinik¹⁸, A. Brandt⁸, G. Brandt⁵⁴, O. Brandt^{58a}, U. Bratzler¹⁵⁶, B. Brau⁸⁶, J. E. Brau¹¹⁶, H. M. Braun^{175,*}, S. F. Brazzale^{164a,164c}, W. D. Breaden Madden⁵³, K. Brendlinger¹²², A. J. Brennan⁸⁸, L. Brenner¹⁰⁷, R. Brenner¹⁶⁶, S. Bressler¹⁷², K. Bristow^{145c}, T. M. Bristow⁴⁶, D. Britton⁵³, D. Britzger⁴², F. M. Brochu²⁸, I. Brock²¹, R. Brock⁹⁰, J. Bronner¹⁰¹, G. Brooijmans³⁵, T. Brooks⁷⁷, W. K. Brooks^{32b}, J. Brosamer¹⁵, E. Brost¹¹⁶, J. Brown⁵⁵, P. A. Bruckman de Renstrom³⁹, D. Bruncko^{144b}, R. Bruneliere⁴⁸, A. Bruni^{20a}, G. Bruni^{20a}, M. Bruschi^{20a}, N. Bruscino²¹, L. Bryngemark⁸¹, T. Buanes¹⁴, Q. Buat¹⁴², P. Buchholz¹⁴¹, A. G. Buckley⁵³, S. I. Buda^{26b}, I. A. Budagov⁶⁵, F. Buehrer⁴⁸, L. Bugge¹¹⁹, M. K. Bugge¹¹⁹, O. Bulekov⁹⁸, D. Bullock⁸, H. Burckhart³⁰, S. Burdin⁷⁴, C. D. Burgard⁴⁸, B. Burghgrave¹⁰⁸, S. Burke¹³¹, I. Burmeister⁴³, E. Busato³⁴, D. Büscher⁴⁸, V. Büscher⁸³, P. Bussey⁵³, J. M. Butler²², A. I. Butt³, C. M. Buttar⁵³, J. M. Butterworth⁷⁸, P. Butti¹⁰⁷, W. Buttinger²⁵, A. Buzatu⁵³, A. R. Buzykaev^{109,c}, S. Cabrera Urbán¹⁶⁷, D. Caforio¹²⁸, V. M. Cairo^{37a,37b}, O. Cakir^{4a}, N. Calace⁴⁹, P. Calafiura¹⁵, A. Calandri¹³⁶, G. Calderini⁸⁰, P. Calfayan¹⁰⁰, L. P. Caloba^{24a}, D. Calvet³⁴, S. Calvet³⁴, R. Camacho Toro³¹, S. Camarda⁴², P. Camarri^{133a,133b}, D. Cameron¹¹⁹, R. Caminal Armadans¹⁶⁵, S. Campana³⁰, M. Campanelli⁷⁸, A. Campoverde¹⁴⁸, V. Canale^{104a,104b}, A. Canepa^{159a}, M. Cano Bret^{33c}, J. Cantero⁸², R. Cantrill^{126a}, T. Cao⁴⁰, M. D. M. Capeans Garrido³⁰, I. Caprini^{26b}, M. Caprini^{26b}, M. Capua^{37a,37b}, R. Caputo⁸³, R. Cardarelli^{133a}, F. Cardillo⁴⁸, T. Carli³⁰, G. Carlino^{104a}, L. Carminati^{91a,91b}, S. Caron¹⁰⁶, E. Carquin^{32a}, G. D. Carrillo-Montoya³⁰, J. R. Carter²⁸, J. Carvalho^{126a,126c}, D. Casadei⁷⁸, M. P. Casado¹², M. Casolino¹², E. Castaneda-Miranda^{145a}, A. Castelli¹⁰⁷, V. Castillo Gimenez¹⁶⁷, N. F. Castro^{126a,g}, P. Catastini⁵⁷, A. Catinaccio³⁰, J. R. Catmore¹¹⁹, A. Cattai³⁰, J. Caudron⁸³, V. Cavaliere¹⁶⁵, D. Cavalli^{91a}, M. Cavalli-Sforza¹², V. Cavasinni^{124a,124b}, F. Ceradini^{134a,134b}, B. C. Cerio⁴⁵, K. Cerny¹²⁹, A. S. Cerqueira^{24b}, A. Cerri¹⁴⁹, L. Cerrito⁷⁶, F. Cerutti¹⁵, M. Cerv³⁰, A. Cervelli¹⁷, S. A. Cetin^{19c}, A. Chafaq^{135a}, D. Chakraborty¹⁰⁸, I. Chalupkova¹²⁹, P. Chang¹⁶⁵, J. D. Chapman²⁸, D. G. Charlton¹⁸, C. C. Chau¹⁵⁸, C. A. Chavez Barajas¹⁴⁹, S. Cheatham¹⁵², A. Chegwidan⁹⁰, S. Chekanov⁶, S. V. Chekulaev^{159a}, G. A. Chelkov^{65,h}, M. A. Chelstowska⁸⁹, C. Chen⁶⁴, H. Chen²⁵, K. Chen¹⁴⁸, L. Chen^{33d,i}, S. Chen^{33c}, S. Chen¹⁵⁵, X. Chen^{33f}, Y. Chen⁶⁷, H. C. Cheng⁸⁹, Y. Cheng³¹, A. Cheplakov⁶⁵, E. Cheremushkina¹³⁰, R. Cherkaoui El Moursli^{135e}, V. Chernyatin^{25,*}, E. Cheu⁷, L. Chevalier¹³⁶, V. Chiarella⁴⁷, G. Chiarelli^{124a,124b}, G. Chiodini^{73a}, A. S. Chisholm¹⁸, R. T. Chislett⁷⁸, A. Chitan^{26b}, M. V. Chizhov⁶⁵, K. Choi⁶¹, S. Chouridou⁹, B. K. B. Chow¹⁰⁰, V. Christodoulou⁷⁸, D. Chromek-Burckhart³⁰, J. Chudoba¹²⁷, A. J. Chuinard⁸⁷, J. J. Chwastowski³⁹, L. Chytka¹¹⁵, G. Ciapetti^{132a,132b}, A. K. Ciftci^{4a}, D. Cinca⁵³, V. Cindro⁷⁵, I. A. Cioara²¹, A. Ciocio¹⁵, F. Ciroto^{104a,104b}, Z. H. Citron¹⁷², M. Ciubancan^{26b}, A. Clark⁴⁹, B. L. Clark⁵⁷, P. J. Clark⁴⁶, R. N. Clarke¹⁵, W. Cleland¹²⁵, C. Clement^{146a,146b}, Y. Coadou⁸⁵, M. Cobal^{164a,164c}, A. Coccaro⁴⁹, J. Cochran⁶⁴, L. Coffey²³, J. G. Cogan¹⁴³, L. Colasurdo¹⁰⁶, B. Cole³⁵, S. Cole¹⁰⁸, A. P. Colijn¹⁰⁷, J. Collot⁵⁵, T. Colombo^{58c}, G. Compostella¹⁰¹, P. Conde Muño^{126a,126b}, E. Coniavitis⁴⁸, S. H. Connell^{145b}, I. A. Connelly⁷⁷, V. Consorti⁴⁸, S. Constantinescu^{26b}, C. Conta^{121a,121b}, G. Conti³⁰, F. Conventi^{104a,j}, M. Cooke¹⁵, B. D. Cooper⁷⁸, A. M. Cooper-Sarkar¹²⁰, T. Cornelissen¹⁷⁵, M. Corradi^{20a}, F. Corriveau^{87,k}, A. Corso-Radu¹⁶³, A. Cortes-Gonzalez¹², G. Cortiana¹⁰¹, G. Costa^{91a}, M. J. Costa¹⁶⁷, D. Costanzo¹³⁹, D. Côté⁸, G. Cottin²⁸, G. Cowan⁷⁷, B. E. Cox⁸⁴, K. Cranmer¹¹⁰, G. Cree²⁹, S. Crépe-Renaudin⁵⁵, F. Crescioli⁸⁰, W. A. Cribbs^{146a,146b}, M. Crispin Ortuzar¹²⁰, M. Cristinziani²¹, V. Croft¹⁰⁶, G. Crosetti^{37a,37b}, T. Cuhadar Donszelmann¹³⁹, J. Cummings¹⁷⁶, M. Curatolo⁴⁷, J. Cúth⁸³, C. Cuthbert¹⁵⁰, H. Czirr¹⁴¹, P. Czodrowski³, S. D'Auria⁵³, M. D'Onofrio⁷⁴, M. J. Da Cunha Sargedas De Sousa^{126a,126b}, C. Da Via⁸⁴, W. Dabrowski^{38a}, A. Dafinca¹²⁰, T. Dai⁸⁹, O. Dale¹⁴, F. Dallaire⁹⁵, C. Dallapiccola⁸⁶, M. Dam³⁶, J. R. Dandoy³¹, N. P. Dang⁴⁸, A. C. Daniells¹⁸, M. Danninger¹⁶⁸, M. Dano Hoffmann¹³⁶, V. Dao⁴⁸, G. Darbo^{50a}, S. Darmora⁸, J. Dassoulas³, A. Dattagupta⁶¹, W. Davey²¹, C. David¹⁶⁹, T. Davidek¹²⁹, E. Davies^{120,l}, M. Davies¹⁵³, P. Davison⁷⁸, Y. Davygora^{58a}, E. Dawe⁸⁸, I. Dawson¹³⁹, R. K. Daya-Ishmukhametova⁸⁶, K. De⁸, R. de Asmundis^{104a}, A. De Benedetti¹¹³, S. De Castro^{20a,20b}, S. De Cecco⁸⁰, N. De Groot¹⁰⁶, P. de Jong¹⁰⁷, H. De la Torre⁸², F. De Lorenzi⁶⁴, D. De Pedis^{132a}, A. De Salvo^{132a}, U. De Sanctis¹⁴⁹, A. De Santo¹⁴⁹, J. B. De Vivie De Regie¹¹⁷, W. J. Dearnaley⁷², R. Debe²⁵, C. Debenedetti¹³⁷, D. V. Dedovich⁶⁵, I. Deigaard¹⁰⁷, J. Del Peso⁸², T. Del Prete^{124a,124b}, D. Delgove¹¹⁷, F. Deliot¹³⁶, C. M. Delitzsch⁴⁹, M. Deliyergiyev⁷⁵, A. Dell'Acqua³⁰, L. Dell'Asta²², M. Dell'Orso^{124a,124b}, M. Della Pietra^{104a,j}, D. della Volpe⁴⁹, M. Delmastro⁵, P. A. Delsart⁵⁵, C. Deluca¹⁰⁷, D. A. DeMarco¹⁵⁸, S. Demers¹⁷⁶, M. Demichev⁶⁵

A. Demilly⁸⁰, S. P. Denisov¹³⁰, D. Derendarz³⁹, J. E. Derkaoui^{135d}, F. Derue⁸⁰, P. Dervan⁷⁴, K. Desch²¹, C. Deterre⁴², P. O. Deviveiros³⁰, A. Dewhurst¹³¹, S. Dhaliwal²³, A. Di Ciaccio^{133a,133b}, L. Di Ciaccio⁵, A. Di Domenico^{132a,132b}, C. Di Donato^{104a,104b}, A. Di Girolamo³⁰, B. Di Girolamo³⁰, A. Di Mattia¹⁵², B. Di Micco^{134a,134b}, R. Di Nardo⁴⁷, A. Di Simone⁴⁸, R. Di Sipio¹⁵⁸, D. Di Valentino²⁹, C. Diaconu⁸⁵, M. Diamond¹⁵⁸, F. A. Dias⁴⁶, M. A. Diaz^{32a}, E. B. Diehl⁸⁹, J. Dietrich¹⁶, S. Diglio⁸⁵, A. Dimitrievska¹³, J. Dingfelder²¹, P. Dita^{26b}, S. Dita^{26b}, F. Dittus³⁰, F. Djama⁸⁵, T. Djobava^{51b}, J. I. Djuvsland^{58a}, M. A. B. do Vale^{24c}, D. Dobos³⁰, M. Dobre^{26b}, C. Doglioni⁸¹, T. Dohmae¹⁵⁵, J. Dolejsi¹²⁹, Z. Dolezal¹²⁹, B. A. Dolgoshein^{98,*}, M. Donadelli^{24d}, S. Donati^{124a,124b}, P. Dondero^{121a,121b}, J. Donini³⁴, J. Dopke¹³¹, A. Doria^{104a}, M. T. Dova⁷¹, A. T. Doyle⁵³, E. Drechsler⁵⁴, M. Dris¹⁰, E. Dubreuil³⁴, E. Duchovni¹⁷², G. Duckeck¹⁰⁰, O. A. Ducu^{26b,85}, D. Duda¹⁰⁷, A. Dudarev³⁰, L. Dufлот¹¹⁷, L. Duguid⁷⁷, M. Dührssen³⁰, M. Dunford^{58a}, H. Duran Yildiz^{4a}, M. Düren⁵², A. Durglishvili^{51b}, D. Duschinger⁴⁴, M. Dyndal^{38a}, C. Eckardt⁴², K. M. Ecker¹⁰¹, R. C. Edgar⁸⁹, W. Edson², N. C. Edwards⁴⁶, W. Ehrenfeld²¹, T. Eifert³⁰, G. Eigen¹⁴, K. Einsweiler¹⁵, T. Ekelif¹⁶⁶, M. El Kacimi^{135c}, M. Ellert¹⁶⁶, S. Elles⁵, F. Ellinghaus¹⁷⁵, A. A. Elliot¹⁶⁹, N. Ellis³⁰, J. Elmsheuser¹⁰⁰, M. Elsing³⁰, D. Emeliyanov¹³¹, Y. Enari¹⁵⁵, O. C. Endner⁸³, M. Endo¹¹⁸, J. Erdmann⁴³, A. Ereditato¹⁷, G. Ernis¹⁷⁵, J. Ernst², M. Ernst²⁵, S. Errede¹⁶⁵, E. Ertel⁸³, M. Escalier¹¹⁷, H. Esch⁴³, C. Escobar¹²⁵, B. Esposito⁴⁷, A. I. Etienvre¹³⁶, E. Etzion¹⁵³, H. Evans⁶¹, A. Ezhilov¹²³, L. Fabbri^{20a,20b}, G. Facini³¹, R. M. Fakhruddinov¹³⁰, S. Falciano^{132a}, R. J. Falla⁷⁸, J. Faltova¹²⁹, Y. Fang^{33a}, M. Fanti^{91a,91b}, A. Farbin⁸, A. Farilla^{134a}, T. Farooque¹², S. Farrell¹⁵, S. M. Farrington¹⁷⁰, P. Farthouat³⁰, F. Fassi^{135e}, P. Fassnacht³⁰, D. Fassouliotis⁹, M. Fauci Giannelli⁷⁷, A. Favareto^{50a,50b}, L. Fayard¹¹⁷, P. Federic^{144a}, O. L. Fedin^{123,m}, W. Fedorko¹⁶⁸, S. Feigl³⁰, L. Feligioni⁸⁵, C. Feng^{33d}, E. J. Feng⁶, H. Feng⁸⁹, A. B. Fenyuk¹³⁰, L. Feremenga⁸, P. Fernandez Martinez¹⁶⁷, S. Fernandez Perez³⁰, J. Ferrando⁵³, A. Ferrari¹⁶⁶, P. Ferrari¹⁰⁷, R. Ferrari^{121a}, D. E. Ferreira de Lima⁵³, A. Ferrer¹⁶⁷, D. Ferrere⁴⁹, C. Ferretti⁸⁹, A. Ferretto Parodi^{50a,50b}, M. Fiascaris³¹, F. Fiedler⁸³, A. Filipčič⁷⁵, M. Filipuzzi⁴², F. Filthaut¹⁰⁶, M. Fincke-Keeler¹⁶⁹, K. D. Finelli¹⁵⁰, M. C. N. Fiolhais^{126a,126c}, L. Fiorini¹⁶⁷, A. Firan⁴⁰, A. Fischer², C. Fischer¹², J. Fischer¹⁷⁵, W. C. Fisher⁹⁰, E. A. Fitzgerald²³, N. Flaschel⁴², I. Fleck¹⁴¹, P. Fleischmann⁸⁹, S. Fleischmann¹⁷⁵, G. T. Fletcher¹³⁹, G. Fletcher⁷⁶, R. R. M. Fletcher¹²², T. Flick¹⁷⁵, A. Floderus⁸¹, L. R. Flores Castillo^{60a}, M. J. Flowerdew¹⁰¹, A. Formica¹³⁶, A. Forti⁸⁴, D. Fournier¹¹⁷, H. Fox⁷², S. Fracchia¹², P. Francavilla⁸⁰, M. Franchini^{20a,20b}, D. Francis³⁰, L. Franconi¹¹⁹, M. Franklin⁵⁷, M. Frate¹⁶³, M. Fraternali^{121a,121b}, D. Freeborn⁷⁸, S. T. French²⁸, F. Friedrich⁴⁴, D. Froidevaux³⁰, J. A. Frost¹²⁰, C. Fukunaga¹⁵⁶, E. Fullana Torregrosa⁸³, B. G. Fulson¹⁴³, T. Fusayasu¹⁰², J. Fuster¹⁶⁷, C. Gabaldon⁵⁵, O. Gabizon¹⁷⁵, A. Gabrielli^{20a,20b}, A. Gabrielli¹⁵, G. P. Gach^{38a}, S. Gadatsch³⁰, S. Gadomski⁴⁹, G. Gagliardi^{50a,50b}, P. Gagnon⁶¹, C. Galea¹⁰⁶, B. Galhardo^{126a,126c}, E. J. Gallas¹²⁰, B. J. Gallop¹³¹, P. Gallus¹²⁸, G. Galster³⁶, K. K. Gan¹¹¹, J. Gao^{33b,85}, Y. Gao⁴⁶, Y. S. Gao^{143,e}, F. M. Garay Walls⁴⁶, F. Garbersson¹⁷⁶, C. García¹⁶⁷, J. E. García Navarro¹⁶⁷, M. Garcia-Sciveres¹⁵, R. W. Gardner³¹, N. Garelli¹⁴³, V. Garonne¹¹⁹, C. Gatti⁴⁷, A. Gaudiello^{50a,50b}, G. Gaudio^{121a}, B. Gaur¹⁴¹, L. Gauthier⁹⁵, P. Gauzzi^{132a,132b}, I. L. Gavrilenko⁹⁶, C. Gay¹⁶⁸, G. Gaycken²¹, E. N. Gazis¹⁰, P. Ge^{33d}, Z. Gece¹⁶⁸, C. N. P. Gee¹³¹, Ch. Geich-Gimbel²¹, M. P. Geisler^{58a}, C. Gemme^{50a}, M. H. Genest⁵⁵, S. Gentile^{132a,132b}, M. George⁵⁴, S. George⁷⁷, D. Gerbaudo¹⁶³, A. Gershon¹⁵³, S. Ghasemi¹⁴¹, H. Ghazlane^{135b}, B. Giacobbe^{20a}, S. Giagu^{132a,132b}, V.angiobbe¹², P. Giannetti^{124a,124b}, B. Gibbard²⁵, S. M. Gibson⁷⁷, M. Gilchriese¹⁵, T. P. S. Gillam²⁸, D. Gillberg³⁰, G. Gilles³⁴, D. M. Gingrich^{3,d}, N. Giokaris⁹, M. P. Giordani^{164a,164c}, F. M. Giorgi^{20a}, F. M. Giorgi¹⁶, P. F. Giraud¹³⁶, P. Giromini⁴⁷, D. Giugni^{91a}, C. Giuliani⁴⁸, M. Giuliani^{58b}, B. K. Gjelsten¹¹⁹, S. Gkaitatzis¹⁵⁴, I. Gkialas¹⁵⁴, E. L. Gkoukousis¹¹⁷, L. K. Gladilin⁹⁹, C. Glasman⁸², J. Glatzer³⁰, P. C. F. Glaysheer⁴⁶, A. Glazov⁴², M. Goblirsch-Kolb¹⁰¹, J. R. Goddard⁷⁶, J. Godlewski³⁹, S. Goldfarb⁸⁹, T. Golling⁴⁹, D. Golubkov¹³⁰, A. Gomes^{126a,126b,126d}, R. Gonçalo^{126a}, J. Goncalves Pinto Firmino Da Costa¹³⁶, L. Gonella²¹, S. González de la Hoz¹⁶⁷, G. Gonzalez Parra¹², S. Gonzalez-Sevilla⁴⁹, L. Goossens³⁰, P. A. Gorbounov⁹⁷, H. A. Gordon²⁵, I. Gorelov¹⁰⁵, B. Gorini³⁰, E. Gorini^{73a,73b}, A. Gorišek⁷⁵, E. Gornicki³⁹, A. T. Goshaw⁴⁵, C. Gössling⁴³, M. I. Gostkin⁶⁵, D. Goujdami^{135c}, A. G. Goussiou¹³⁸, N. Govender^{145b}, E. Gozani¹⁵², H. M. X. Grabas¹³⁷, L. Graber⁵⁴, I. Grabowska-Bold^{38a}, P. O. J. Gradin¹⁶⁶, P. Grafström^{20a,20b}, K.-J. Grahn⁴², J. Gramling⁴⁹, E. Gramstad¹¹⁹, S. Grancagnolo¹⁶, V. Gratchev¹²³, H. M. Gray³⁰, E. Graziani^{134a}, Z. D. Greenwood^{79,n}, C. Grefe²¹, K. Gregersen⁷⁸, I. M. Gregor⁴², P. Grenier¹⁴³, J. Griffiths⁸, A. A. Grillo¹³⁷, K. Grimm⁷², S. Grinstein^{12,o}, Ph. Gris³⁴, J.-F. Grivaz¹¹⁷, J. P. Grohs⁴⁴, A. Grohsjean⁴², E. Gross¹⁷², J. Grosse-Knetter⁵⁴, G. C. Grossi⁷⁹, Z. J. Grout¹⁴⁹, L. Guan⁸⁹, J. Guenther¹²⁸, F. Guescini⁴⁹, D. Guest¹⁷⁶, O. Gueta¹⁵³, E. Guido^{50a,50b}, T. Guillemin¹¹⁷, S. Guindon², U. Gul⁵³, C. Gumpert⁴⁴, J. Guo^{33e}, Y. Guo^{33b}, S. Gupta¹²⁰, G. Gustavino^{132a,132b}, P. Gutierrez¹¹³, N. G. Gutierrez Ortiz⁷⁸, C. Gutschow⁴⁴, C. Guyot¹³⁶, C. Gwenlan¹²⁰, C. B. Gwilliam⁷⁴, A. Haas¹¹⁰, C. Haber¹⁵, H. K. Hadavand⁸, N. Haddad^{135e}, P. Haefner²¹, S. Hageböck²¹, Z. Hajduk³⁹, H. Hakobyan¹⁷⁷, M. Haleem⁴², J. Haley¹¹⁴, D. Hall¹²⁰, G. Halladjian⁹⁰, G. D. Hallewell⁸⁵, K. Hamacher¹⁷⁵, P. Hamal¹¹⁵, K. Hamano¹⁶⁹, A. Hamilton^{145a}, G. N. Hamity¹³⁹, P. G. Hamnett⁴², L. Han^{33b}, K. Hanagaki^{66,p}, K. Hanawa¹⁵⁵, M. Hance¹⁵, B. Haney¹²², P. Hanke^{58a}, R. Hanna¹³⁶, J. B. Hansen³⁶, J. D. Hansen³⁶, M. C. Hansen²¹, P. H. Hansen³⁶, K. Hara¹⁶⁰, A. S. Hard¹⁷³, T. Harenberg¹⁷⁵, F. Hariri¹¹⁷, S. Harkusha⁹²

R. D. Harrington⁴⁶, P. F. Harrison¹⁷⁰, F. Hartjes¹⁰⁷, M. Hasegawa⁶⁷, Y. Hasegawa¹⁴⁰, A. Hasib¹¹³, S. Hassani¹³⁶, S. Haug¹⁷, R. Hauser⁹⁰, L. Hauswald⁴⁴, M. Havranek¹²⁷, C. M. Hawkes¹⁸, R. J. Hawkins³⁰, A. D. Hawkins⁸¹, T. Hayashi¹⁶⁰, D. Hayden⁹⁰, C. P. Hays¹²⁰, J. M. Hays⁷⁶, H. S. Hayward⁷⁴, S. J. Haywood¹³¹, S. J. Head¹⁸, T. Heck⁸³, V. Hedberg⁸¹, L. Heelan⁸, S. Heim¹²², T. Heim¹⁷⁵, B. Heinemann¹⁵, L. Heinrich¹¹⁰, J. Hejbal¹²⁷, L. Helary²², S. Hellman^{146a,146b}, D. Hellmich²¹, C. Helsens¹², J. Henderson¹²⁰, R. C. W. Henderson⁷², Y. Heng¹⁷³, C. Hengler⁴², S. Henkelmann¹⁶⁸, A. Henrichs¹⁷⁶, A. M. Henriques Correia³⁰, S. Henrot-Versille¹¹⁷, G. H. Herbert¹⁶, Y. Hernández Jiménez¹⁶⁷, R. Herrberg-Schubert¹⁶, G. Herten⁴⁸, R. Hertenberger¹⁰⁰, L. Hervas³⁰, G. G. Hesketh⁷⁸, N. P. Hessey¹⁰⁷, J. W. Hetherly⁴⁰, R. Hickling⁷⁶, E. Higón-Rodríguez¹⁶⁷, E. Hill¹⁶⁹, J. C. Hill²⁸, K. H. Hiller⁴², S. J. Hillier¹⁸, I. Hinchliffe¹⁵, E. Hines¹²², R. R. Hinman¹⁵, M. Hirose¹⁵⁷, D. Hirschbuehl¹⁷⁵, J. Hobbs¹⁴⁸, N. Hod¹⁰⁷, M. C. Hodgkinson¹³⁹, P. Hodgson¹³⁹, A. Hoecker³⁰, M. R. Hoferkamp¹⁰⁵, F. Hoenig¹⁰⁰, M. Hohlfeld⁸³, D. Hohn²¹, T. R. Holmes¹⁵, M. Homann⁴³, T. M. Hong¹²⁵, L. Hooft van Huysduynen¹¹⁰, W. H. Hopkins¹¹⁶, Y. Horii¹⁰³, A. J. Horton¹⁴², J.-Y. Hostachy⁵⁵, S. Hou¹⁵¹, A. Houmada^{135a}, J. Howard¹²⁰, J. Howarth⁴², M. Hrabovsky¹¹⁵, I. Hristova¹⁶, J. Hrivnac¹¹⁷, T. Hryn'ova⁵, A. Hrynevich⁹³, C. Hsu^{145c}, P. J. Hsu^{151,q}, S.-C. Hsu¹³⁸, D. Hu³⁵, Q. Hu^{33b}, X. Hu⁸⁹, Y. Huang⁴², Z. Hubacek¹²⁸, F. Hubaut⁸⁵, F. Huegging²¹, T. B. Huffman¹²⁰, E. W. Hughes³⁵, G. Hughes⁷², M. Huhtinen³⁰, T. A. Hülsing⁸³, N. Huseynov^{65,b}, J. Huston⁹⁰, J. Huth⁵⁷, G. Iacobucci⁴⁹, G. Iakovidis²⁵, I. Ibragimov¹⁴¹, L. Iconomidou-Fayard¹¹⁷, E. Ideal¹⁷⁶, Z. Idrissi^{135c}, P. Iengo³⁰, O. Igonkina¹⁰⁷, T. Iizawa¹⁷¹, Y. Ikegami⁶⁶, K. Ikematsu¹⁴¹, M. Ikeno⁶⁶, Y. Ilchenko^{31,r}, D. Iliadis¹⁵⁴, N. Ilic¹⁴³, T. Ince¹⁰¹, G. Introzzi^{121a,121b}, P. Ioannou⁹, M. Iodice^{134a}, K. Iordanidou³⁵, V. Ippolito⁵⁷, A. Irlés Quiles¹⁶⁷, C. Isaksson¹⁶⁶, M. Ishino⁶⁸, M. Ishitsuka¹⁵⁷, R. Ishmukhametov¹¹¹, C. Issever¹²⁰, S. Istin^{19a}, J. M. Iturbe Ponce⁸⁴, R. Iuppa^{133a,133b}, J. Ivarsson⁸¹, W. Iwanski³⁹, H. Iwasaki⁶⁶, J. M. Izen⁴¹, V. Izzo^{104a}, S. Jabbar³, B. Jackson¹²², M. Jackson⁷⁴, P. Jackson¹, M. R. Jaekel³⁰, V. Jain², K. Jakobs⁴⁸, S. Jakobsen³⁰, T. Jakoubek¹²⁷, J. Jakubek¹²⁸, D. O. Jamin¹¹⁴, D. K. Jana⁷⁹, E. Jansen⁷⁸, R. Jansky⁶², J. Janssen²¹, M. Janus⁵⁴, G. Jarlskog⁸¹, N. Javadov^{65,b}, T. Javůrek⁴⁸, L. Jeanty¹⁵, J. Jejelava^{51a,s}, G.-Y. Jeng¹⁵⁰, D. Jennens⁸⁸, P. Jenni^{48,t}, J. Jentzsch⁴³, C. Jeske¹⁷⁰, S. Jézéquel⁵, H. Ji¹⁷³, J. Jia¹⁴⁸, Y. Jiang^{33b}, S. Jiggins⁷⁸, J. Jimenez Pena¹⁶⁷, S. Jin^{33a}, A. Jinaru^{26b}, O. Jinnouchi¹⁵⁷, M. D. Joergensen³⁶, P. Johansson¹³⁹, K. A. Johns⁷, K. Jon-And^{146a,146b}, G. Jones¹⁷⁰, R. W. L. Jones⁷², T. J. Jones⁷⁴, J. Jongmanns^{58a}, P. M. Jorge^{126a,126b}, K. D. Joshi⁸⁴, J. Jovicevic^{159a}, X. Ju¹⁷³, C. A. Jung⁴³, P. Jussel⁶², A. Juste Rozas^{12,o}, M. Kaci¹⁶⁷, A. Kaczmarska³⁹, M. Kado¹¹⁷, H. Kagan¹¹¹, M. Kagan¹⁴³, S. J. Kahn⁸⁵, E. Kajomovitz⁴⁵, C. W. Kalderon¹²⁰, S. Kama⁴⁰, A. Kamenshchikov¹³⁰, N. Kanaya¹⁵⁵, S. Kaneti²⁸, V. A. Kantserov⁹⁸, J. Kanzaki⁶⁶, B. Kaplan¹¹⁰, L. S. Kaplan¹⁷³, A. Kapliy³¹, D. Kar^{145c}, K. Karakostas¹⁰, A. Karamaoun³, N. Karastathis^{10,107}, M. J. Kareem⁵⁴, E. Karentzos¹⁰, M. Karnevskiy⁸³, S. N. Karpov⁶⁵, Z. M. Karpova⁶⁵, K. Karthik¹¹⁰, V. Kartvelishvili⁷², A. N. Karyukhin¹³⁰, K. Kasahara¹⁶⁰, L. Kashif¹⁷³, R. D. Kass¹¹¹, A. Kastanas¹⁴, Y. Kataoka¹⁵⁵, C. Kato¹⁵⁵, A. Katre⁴⁹, J. Katzy⁴², K. Kawagoe⁷⁰, T. Kawamoto¹⁵⁵, G. Kawamura⁵⁴, S. Kazama¹⁵⁵, V. F. Kazanin^{109,c}, R. Keeler¹⁶⁹, R. Kehoe⁴⁰, J. S. Keller⁴², J. J. Kempster⁷⁷, H. Keoshkerian⁸⁴, O. Kepka¹²⁷, B. P. Kerševan⁷⁵, S. Kersten¹⁷⁵, R. A. Keyes⁸⁷, F. Khalil-zada¹¹, H. Khandanyan^{146a,146b}, A. Khanov¹¹⁴, A. G. Kharlamov^{109,c}, T. J. Khoo²⁸, V. Khovanskii⁹⁷, E. Khramov⁶⁵, J. Khubua^{51b,u}, S. Kido⁶⁷, H. Y. Kim⁸, S. H. Kim¹⁶⁰, Y. K. Kim³¹, N. Kimura¹⁵⁴, O. M. Kind¹⁶, B. T. King⁷⁴, M. King¹⁶⁷, S. B. King¹⁶⁸, J. Kirk¹³¹, A. E. Kiryunin¹⁰¹, T. Kishimoto⁶⁷, D. Kisielewska^{38a}, F. Kiss⁴⁸, K. Kiuchi¹⁶⁰, O. Kivernyk¹³⁶, E. Kladiva^{144b}, M. H. Klein³⁵, M. Klein⁷⁴, U. Klein⁷⁴, K. Kleinknecht⁸³, P. Klimek^{146a,146b}, A. Klimentov²⁵, R. Klingenberg⁴³, J. A. Klinger¹³⁹, T. Klioutchnikova³⁰, E.-E. Kluge^{58a}, P. Kluit¹⁰⁷, S. Kluth¹⁰¹, J. Knapik³⁹, E. Kneringer⁶², E. B. F. G. Knoops⁸⁵, A. Knue⁵³, A. Kobayashi¹⁵⁵, D. Kobayashi¹⁵⁷, T. Kobayashi¹⁵⁵, M. Kobel⁴⁴, M. Kocian¹⁴³, P. Kodys¹²⁹, T. Koffas²⁹, E. Koffeman¹⁰⁷, L. A. Kogan¹²⁰, S. Kohlmann¹⁷⁵, Z. Kohout¹²⁸, T. Kohriki⁶⁶, T. Koi¹⁴³, H. Kolanoski¹⁶, I. Koletsou⁵, A. A. Komar^{96,*}, Y. Komori¹⁵⁵, T. Kondo⁶⁶, N. Kondrashova⁴², K. Köneke⁴⁸, A. C. König¹⁰⁶, T. Kono⁶⁶, R. Konoplich^{110,v}, N. Konstantinidis⁷⁸, R. Kopeliansky¹⁵², S. Koperny^{38a}, L. Köpke⁸³, A. K. Kopp⁴⁸, K. Korcyl³⁹, K. Kordas¹⁵⁴, A. Korn⁷⁸, A. A. Korol^{109,c}, I. Korolkov¹², E. V. Korolkova¹³⁹, O. Kortner¹⁰¹, S. Kortner¹⁰¹, T. Kosek¹²⁹, V. V. Kostyukhin²¹, V. M. Kotov⁶⁵, A. Kotwal⁴⁵, A. Kourkoumeli-Charalampidi¹⁵⁴, C. Kourkoumelis⁹, V. Kouskoura²⁵, A. Koutsman^{159a}, R. Kowalewski¹⁶⁹, T. Z. Kowalski^{38a}, W. Kozanecki¹³⁶, A. S. Kozhin¹³⁰, V. A. Kramarenko⁹⁹, G. Kramberger⁷⁵, D. Krasnopevtsev⁹⁸, M. W. Krasny⁸⁰, A. Krasznahorkay³⁰, J. K. Kraus²¹, A. Kravchenko²⁵, S. Kreiss¹¹⁰, M. Kretz^{58c}, J. Kretzschmar⁷⁴, K. Kreutzfeldt⁵², P. Krieger¹⁵⁸, K. Krizka³¹, K. Kroeninger⁴³, H. Kroha¹⁰¹, J. Kroll¹²², J. Kroseberg²¹, J. Krstic¹³, U. Kruchonak⁶⁵, H. Krüger²¹, N. Krumnack⁶⁴, A. Kruse¹⁷³, M. C. Kruse⁴⁵, M. Kruskal²², T. Kubota⁸⁸, H. Kucuk⁷⁸, S. Kuday^{4b}, S. Kuehn⁴⁸, A. Kugel^{58c}, F. Kuger¹⁷⁴, A. Kuhl¹³⁷, T. Kuhl⁴², V. Kukhtin⁶⁵, R. Kukla¹³⁶, Y. Kulchitsky⁹², S. Kuleshov^{32b}, M. Kuna^{132a,132b}, T. Kunigo⁶⁸, A. Kupco¹²⁷, H. Kurashige⁶⁷, Y. A. Kurochkin⁹², V. Kus¹²⁷, E. S. Kuwertz¹⁶⁹, M. Kuze¹⁵⁷, J. Kvita¹¹⁵, T. Kwan¹⁶⁹, D. Kyriazopoulos¹³⁹, A. La Rosa¹³⁷, J. L. La Rosa Navarro^{24d}, L. La Rotonda^{37a,37b}, C. Lacasta¹⁶⁷, F. Lacava^{132a,132b}, J. Lacey²⁹, H. Lacker¹⁶, D. Lacour⁸⁰, V. R. Lacuesta¹⁶⁷, E. Ladygin⁶⁵, R. Lafaye⁵, B. Laforge⁸⁰, T. Lagouri¹⁷⁶, S. Lai⁵⁴, L. Lambourne⁷⁸, S. Lammers⁶¹, C. L. Lampen⁷,

W. Lampl⁷, E. Lançon¹³⁶, U. Landgraf⁴⁸, M. P. J. Landon⁷⁶, V. S. Lang^{58a}, J. C. Lange¹², A. J. Lankford¹⁶³, F. Lanni²⁵, K. Lantzsch²¹, A. Lanza^{121a}, S. Laplace⁸⁰, C. Lapoire³⁰, J. F. Laporte¹³⁶, T. Lari^{91a}, F. Lasagni Manghi^{20a,20b}, M. Lassnig³⁰, P. Laurelli⁴⁷, W. Lavrijsen¹⁵, A. T. Law¹³⁷, P. Laycock⁷⁴, T. Lazovich⁵⁷, O. Le Dortz⁸⁰, E. Le Guirriec⁸⁵, E. Le Menedeu¹², M. LeBlanc¹⁶⁹, T. LeCompte⁶, F. Ledroit-Guillon⁵⁵, C. A. Lee^{145b}, S. C. Lee¹⁵¹, L. Lee¹, G. Lefebvre⁸⁰, M. Lefebvre¹⁶⁹, F. Legger¹⁰⁰, C. Leggett¹⁵, A. Lehan⁷⁴, G. Lehmann Miotto³⁰, X. Lei⁷, W. A. Leight²⁹, A. Leisos^{154.w}, A. G. Leister¹⁷⁶, M. A. L. Leite^{24d}, R. Leitner¹²⁹, D. Lellouch¹⁷², B. Lemmer⁵⁴, K. J. C. Leney⁷⁸, T. Lenz²¹, B. Lenzi³⁰, R. Leone⁷, S. Leone^{124a,124b}, C. Leonidopoulos⁴⁶, S. Leontsinis¹⁰, C. Leroy⁹⁵, C. G. Lester²⁸, M. Levchenko¹²³, J. Levêque⁵, D. Levin⁸⁹, L. J. Levinson¹⁷², M. Levy¹⁸, A. Lewis¹²⁰, A. M. Leyko²¹, M. Leyton⁴¹, B. Li^{33b,x}, H. Li¹⁴⁸, H. L. Li³¹, L. Li⁴⁵, L. Li^{33e}, S. Li⁴⁵, X. Li⁸⁴, Y. Li^{33c,y}, Z. Liang¹³⁷, H. Liao³⁴, B. Liberti^{133a}, A. Liblong¹⁵⁸, P. Lichard³⁰, K. Lie¹⁶⁵, J. Liebal²¹, W. Liebig¹⁴, C. Limbach²¹, A. Limosani¹⁵⁰, S. C. Lin^{151,z}, T. H. Lin⁸³, F. Linde¹⁰⁷, B. E. Lindquist¹⁴⁸, J. T. Linnemann⁹⁰, E. Lipeles¹²², A. Lipniacka¹⁴, M. Lisovyi^{58b}, T. M. Liss¹⁶⁵, D. Lissauer²⁵, A. Lister¹⁶⁸, A. M. Litke¹³⁷, B. Liu^{151,aa}, D. Liu¹⁵¹, H. Liu⁸⁹, J. Liu⁸⁵, J. B. Liu^{33b}, K. Liu⁸⁵, L. Liu¹⁶⁵, M. Liu⁴⁵, M. Liu^{33b}, Y. Liu^{33b}, M. Livan^{121a,121b}, A. Lleres⁵⁵, J. Llorente Merino⁸², S. L. Lloyd⁷⁶, F. Lo Sterzo¹⁵¹, E. Lobodzinska⁴², P. Loch⁷, W. S. Lockman¹³⁷, F. K. Loebinger⁸⁴, A. E. Loeschall-Jensen³⁶, K. M. Loew²³, A. Loginov¹⁷⁶, T. Lohse¹⁶, K. Lohwasser⁴², M. Lokajicek¹²⁷, B. A. Long²², J. D. Long⁸⁹, R. E. Long⁷², K. A. Looper¹¹¹, L. Lopes^{126a}, D. Lopez Mateos⁵⁷, B. Lopez Paredes¹³⁹, I. Lopez Paz¹², J. Lorenz¹⁰⁰, N. Lorenzo Martinez⁶¹, M. Losada¹⁶², P. J. Lösel¹⁰⁰, X. Lou^{33a}, A. Lounis¹¹⁷, J. Love⁶, P. A. Love⁷², N. Lu⁸⁹, H. J. Lubatti¹³⁸, C. Luci^{132a,132b}, A. Lucotte⁵⁵, F. Luehring⁶¹, W. Lukas⁶², L. Luminari^{132a}, O. Lundberg^{146a,146b}, B. Lund-Jensen¹⁴⁷, D. Lynn²⁵, R. Lysak¹²⁷, E. Lytken⁸¹, H. Ma²⁵, L. L. Ma^{33d}, G. Maccarrone⁴⁷, A. Macchiolo¹⁰¹, C. M. Macdonald¹³⁹, B. Maček⁷⁵, J. Machado Miguens^{122,126b}, D. Macina³⁰, D. Madaffari⁸⁵, R. Madar³⁴, H. J. Maddocks⁷², W. F. Mader⁴⁴, A. Madsen¹⁶⁶, J. Maeda⁶⁷, S. Maeland¹⁴, T. Maeno²⁵, A. Maevskiy⁹⁹, E. Magradze⁵⁴, K. Mahboubi⁴⁸, J. Mahlstedt¹⁰⁷, C. Maiani¹³⁶, C. Maidantchik^{24a}, A. A. Maier¹⁰¹, T. Maier¹⁰⁰, A. Maio^{126a,126b,126d}, S. Majewski¹¹⁶, Y. Makida⁶⁶, N. Makovec¹¹⁷, B. Malaescu⁸⁰, Pa. Malecki³⁹, V. P. Maleev¹²³, F. Malek⁵⁵, U. Mallik⁶³, D. Malon⁶, C. Malone¹⁴³, S. Maltezos¹⁰, V. M. Malyshev¹⁰⁹, S. Malyukov³⁰, J. Mamuzic⁴², G. Mancini⁴⁷, B. Mandelli³⁰, L. Mandelli^{91a}, I. Mandić⁷⁵, R. Mandrysch⁶³, J. Maneira^{126a,126b}, A. Manfredini¹⁰¹, L. Manhaes de Andrade Filho^{24b}, J. Manjarres Ramos^{159b}, A. Mann¹⁰⁰, A. Manousakis-Katsikakis⁹, B. Mansoulie¹³⁶, R. Mantifel⁸⁷, M. Mantoani⁵⁴, L. Mapelli³⁰, L. March^{145c}, G. Marchiori⁸⁰, M. Marcisovsky¹²⁷, C. P. Marino¹⁶⁹, M. Marjanovic¹³, D. E. Marley⁸⁹, F. Marroquim^{24a}, S. P. Marsden⁸⁴, Z. Marshall¹⁵, L. F. Marti¹⁷, S. Marti-Garcia¹⁶⁷, B. Martin⁹⁰, T. A. Martin¹⁷⁰, V. J. Martin⁴⁶, B. Martin dit Latour¹⁴, M. Martinez^{12,o}, S. Martin-Haugh¹³¹, V. S. Martoiu^{26b}, A. C. Martyniuk⁷⁸, M. Marx¹³⁸, F. Marzano^{132a}, A. Marzin³⁰, L. Masetti⁸³, T. Mashimo¹⁵⁵, R. Mashinistov⁹⁶, J. Masik⁸⁴, A. L. Maslennikov^{109,c}, I. Massa^{20a,20b}, L. Massa^{20a,20b}, P. Mastrandrea¹⁴⁸, A. Mastroberardino^{37a,37b}, T. Masubuchi¹⁵⁵, P. Mättig¹⁷⁵, J. Mattmann⁸³, J. Maurer^{26b}, S. J. Maxfield⁷⁴, D. A. Maximov^{109,c}, R. Mazini¹⁵¹, S. M. Mazza^{91a,91b}, L. Mazzaferro^{133a,133b}, G. Mc Goldrick¹⁵⁸, S. P. Mc Kee⁸⁹, A. McCarn⁸⁹, R. L. McCarthy¹⁴⁸, T. G. McCarthy²⁹, N. A. McCubbin¹³¹, K. W. McFarlane^{56,*}, J. A. McFayden⁷⁸, G. Mchedlidze⁵⁴, S. J. McMahon¹³¹, R. A. McPherson^{169,k}, M. Medinnis⁴², S. Meehan^{145a}, S. Mehlhase¹⁰⁰, A. Mehta⁷⁴, K. Meier^{58a}, C. Meineck¹⁰⁰, B. Meirose⁴¹, B. R. Mellado Garcia^{145c}, F. Meloni¹⁷, A. Mengarelli^{20a,20b}, S. Menke¹⁰¹, E. Meoni¹⁶¹, K. M. Mercurio⁵⁷, S. Mergelmeyer²¹, P. Mermod⁴⁹, L. Merola^{104a,104b}, C. Meroni^{91a}, F. S. Merritt³¹, A. Messina^{132a,132b}, J. Metcalfe²⁵, A. S. Mete¹⁶³, C. Meyer⁸³, C. Meyer¹²², J-P. Meyer¹³⁶, J. Meyer¹⁰⁷, H. Meyer Zu Theenhausen^{58a}, R. P. Middleton¹³¹, S. Miglioranza^{164a,164c}, L. Mijović²¹, G. Mikenberg¹⁷², M. Mikestikova¹²⁷, M. Mikuz⁷⁵, M. Milesi⁸⁸, A. Milic³⁰, D. W. Miller³¹, C. Mills⁴⁶, A. Milov¹⁷², D. A. Milstead^{146a,146b}, A. A. Minaenko¹³⁰, Y. Minami¹⁵⁵, I. A. Minashvili⁶⁵, A. I. Mincer¹¹⁰, B. Mindur^{38a}, M. Mineev⁶⁵, Y. Ming¹⁷³, L. M. Mir¹², K. P. Mistry¹²², T. Mitani¹⁷¹, J. Mitrevski¹⁰⁰, V. A. Mitsou¹⁶⁷, A. Miucci⁴⁹, P. S. Miyagawa¹³⁹, J. U. Mjörnmark⁸¹, T. Moa^{146a,146b}, K. Mochizuki⁸⁵, S. Mohapatra³⁵, W. Mohr⁴⁸, S. Molander^{146a,146b}, R. Moles-Valls²¹, R. Monden⁶⁸, K. Mönig⁴², C. Monini⁵⁵, J. Monk³⁶, E. Monnier⁸⁵, J. Montejo Berlingen¹², F. Monticelli⁷¹, S. Monzani^{132a,132b}, R. W. Moore³, N. Morange¹¹⁷, D. Moreno¹⁶², M. Moreno Llácer⁵⁴, P. Morettini^{50a}, D. Mori¹⁴², T. Mori¹⁵⁵, M. Morii⁵⁷, M. Morinaga¹⁵⁵, V. Morisbak¹¹⁹, S. Moritz⁸³, A. K. Morley¹⁵⁰, G. Mornacchi³⁰, J. D. Morris⁷⁶, S. S. Mortensen³⁶, A. Morton⁵³, L. Morvaj¹⁰³, M. Mosidze^{51b}, J. Moss¹⁴³, K. Motohashi¹⁵⁷, R. Mount¹⁴³, E. Mountricha²⁵, S. V. Mouraviev^{96,*}, E. J. W. Moyses⁸⁶, S. Muanza⁸⁵, R. D. Mudd¹⁸, F. Mueller¹⁰¹, J. Mueller¹²⁵, R. S. P. Mueller¹⁰⁰, T. Mueller²⁸, D. Muenstermann⁴⁹, P. Mullen⁵³, G. A. Mullier¹⁷, J. A. Murillo Quijada¹⁸, W. J. Murray^{170,131}, H. Musheghyan⁵⁴, E. Musto¹⁵², A. G. Myagkov^{130,ab}, M. Myska¹²⁸, B. P. Nachman¹⁴³, O. Nackenhorst⁵⁴, J. Nadal⁵⁴, K. Nagai¹²⁰, R. Nagai¹⁵⁷, Y. Nagai⁸⁵, K. Nagano⁶⁶, A. Nagarkar¹¹¹, Y. Nagasaka⁵⁹, K. Nagata¹⁶⁰, M. Nagel¹⁰¹, E. Nagy⁸⁵, A. M. Nairz³⁰, Y. Nakahama³⁰, K. Nakamura⁶⁶, T. Nakamura¹⁵⁵, I. Nakano¹¹², H. Namasivayam⁴¹, R. F. Naranjo Garcia⁴², R. Narayan³¹, D. I. Narrias Villar^{58a}, T. Naumann⁴², G. Navarro¹⁶², R. Nayyar⁷, H. A. Neal⁸⁹, P. Yu. Nechaeva⁹⁶, T. J. Neep⁸⁴, P. D. Nef¹⁴³, A. Negri^{121a,121b}, M. Negrini^{20a}, S. Nektarijevic¹⁰⁶, C. Nellist¹¹⁷, A. Nelson¹⁶³, S. Nemecek¹²⁷, P. Nemethy¹¹⁰, A. A. Nepomuceno^{24a},

M. Nessi^{30,ac}, M. S. Neubauer¹⁶⁵, M. Neumann¹⁷⁵, R. M. Neves¹¹⁰, P. Nevski²⁵, P. R. Newman¹⁸, D. H. Nguyen⁶, R. B. Nickerson¹²⁰, R. Nicolaidou¹³⁶, B. Nicquevert³⁰, J. Nielsen¹³⁷, N. Nikiforou³⁵, A. Nikiforov¹⁶, V. Nikolaenko^{130,ab}, I. Nikolic-Audit⁸⁰, K. Nikolopoulos¹⁸, J. K. Nilsen¹¹⁹, P. Nilsson²⁵, Y. Ninomiya¹⁵⁵, A. Nisati^{132a}, R. Nisius¹⁰¹, T. Nobe¹⁵⁵, M. Nomachi¹¹⁸, I. Nomidis²⁹, T. Nooney⁷⁶, S. Norberg¹¹³, M. Nordberg³⁰, O. Novgorodova⁴⁴, S. Nowak¹⁰¹, M. Nozaki⁶⁶, L. Nozka¹¹⁵, K. Ntekas¹⁰, G. Nunes Hanninger⁸⁸, T. Nunnemann¹⁰⁰, E. Nurse⁷⁸, F. Nuti⁸⁸, B. J. O'Brien⁴⁶, F. O'grady⁷, D. C. O'Neil¹⁴², V. O'Shea⁵³, F. G. Oakham^{29,d}, H. Oberlack¹⁰¹, T. Obermann²¹, J. Ocariz⁸⁰, A. Ochi⁶⁷, I. Ochoa⁷⁸, J. P. Ochoa-Ricoux^{32a}, S. Oda⁷⁰, S. Odaka⁶⁶, H. Ogren⁶¹, A. Oh⁸⁴, S. H. Oh⁴⁵, C. C. Ohm¹⁵, H. Ohman¹⁶⁶, H. Oide³⁰, W. Okamura¹¹⁸, H. Okawa¹⁶⁰, Y. Okumura³¹, T. Okuyama⁶⁶, A. Olariu^{26b}, S. A. Olivares Pino⁴⁶, D. Oliveira Damazio²⁵, E. Oliver Garcia¹⁶⁷, A. Olszewski³⁹, J. Olszowska³⁹, A. Onofre^{126a,126c}, K. Onogi¹⁰³, P. U. E. Onyisi^{31,r}, C. J. Oram^{159a}, M. J. Oreglia³¹, Y. Oren¹⁵³, D. Orestano^{134a,134b}, N. Orlando¹⁵⁴, C. Oropeza Barrera⁵³, R. S. Orr¹⁵⁸, B. Osculati^{50a,50b}, R. Ospanov⁸⁴, G. Otero y Garzon²⁷, H. Otono⁷⁰, M. Ouchrif^{135d}, F. Ould-Saada¹¹⁹, A. Ouraou¹³⁶, K. P. Oussoren¹⁰⁷, Q. Ouyang^{33a}, A. Ovcharova¹⁵, M. Owen⁵³, R. E. Owen¹⁸, V. E. Ozcan^{19a}, N. Ozturk⁸, K. Pachal¹⁴², A. Pacheco Pages¹², C. Padilla Aranda¹², M. Pagáčová⁴⁸, S. Pagan Griso¹⁵, E. Paganis¹³⁹, F. Paige²⁵, P. Pais⁸⁶, K. Pajchel¹¹⁹, G. Palacino^{159b}, S. Palestini³⁰, M. Palka^{38b}, D. Pallin³⁴, A. Palma^{126a,126b}, Y. B. Pan¹⁷³, E. Panagiotopoulou¹⁰, C. E. Pandini⁸⁰, J. G. Panduro Vazquez⁷⁷, P. Pani^{146a,146b}, S. Panitkin²⁵, D. Pantea^{26b}, L. Paolozzi⁴⁹, Th. D. Papadopoulou¹⁰, K. Papageorgiou¹⁵⁴, A. Paramonov⁶, D. Paredes Hernandez¹⁵⁴, M. A. Parker²⁸, K. A. Parker¹³⁹, F. Parodi^{50a,50b}, J. A. Parsons³⁵, U. Parzefall⁴⁸, E. Pasqualucci^{132a}, S. Passaggio^{50a}, F. Pastore^{134a,134b,*}, Fr. Pastore⁷⁷, G. Pásztor²⁹, S. Patariaia¹⁷⁵, N. D. Patel¹⁵⁰, J. R. Pater⁸⁴, T. Pauly³⁰, J. Pearce¹⁶⁹, B. Pearson¹¹³, L. E. Pedersen³⁶, M. Pedersen¹¹⁹, S. Pedraza Lopez¹⁶⁷, R. Pedro^{126a,126b}, S. V. Peleganchuk^{109,c}, D. Pelikan¹⁶⁶, O. Penc¹²⁷, C. Peng^{33a}, H. Peng^{33b}, B. Penning³¹, J. Penwell⁶¹, D. V. Perepelitsa²⁵, E. Perez Codina^{159a}, M. T. Pérez García-Están¹⁶⁷, L. Perini^{91a,91b}, H. Pernegger³⁰, S. Perrella^{104a,104b}, R. Peschke⁴², V. D. Peshekhonov⁶⁵, K. Peters³⁰, R. F. Y. Peters⁸⁴, B. A. Petersen³⁰, T. C. Petersen³⁶, E. Petit⁴², A. Petridis¹, C. Petridou¹⁵⁴, P. Petroff¹¹⁷, E. Petrolu^{132a}, F. Petrucci^{134a,134b}, N. E. Pettersson¹⁵⁷, R. Pezoa^{32b}, P. W. Phillips¹³¹, G. Piacquadio¹⁴³, E. Pianori¹⁷⁰, A. Picazio⁴⁹, E. Piccaro⁷⁶, M. Piccinini^{20a,20b}, M. A. Pickering¹²⁰, R. Piegai²⁷, D. T. Pignotti¹¹¹, J. E. Pilcher³¹, A. D. Pilkington⁸⁴, J. Pina^{126a,126b,126d}, M. Pinamonti^{164a,164c,ad}, J. L. Pinfold³, A. Pingel³⁶, S. Pires⁸⁰, H. Pirumov⁴², M. Pitt¹⁷², C. Pizio^{91a,91b}, L. Plazak^{144a}, M.-A. Pleier²⁵, V. Pleskot¹²⁹, E. Plotnikova⁶⁵, P. Plucinski^{146a,146b}, D. Pluth⁶⁴, R. Poettgen^{146a,146b}, L. Poggioli¹¹⁷, D. Pohl²¹, G. Polesello^{121a}, A. Poley⁴², A. Policicchio^{37a,37b}, R. Polifka¹⁵⁸, A. Polini^{20a}, C. S. Pollard⁵³, V. Polychronakos²⁵, K. Pommès³⁰, L. Pontecorvo^{132a}, B. G. Pope⁹⁰, G. A. Popeneciu^{26c}, D. S. Popovic¹³, A. Poppleton³⁰, S. Pospisil¹²⁸, K. Potamianos¹⁵, I. N. Potrap⁶⁵, C. J. Potter¹⁴⁹, C. T. Potter¹¹⁶, G. Poulard³⁰, J. Poveda³⁰, V. Pozdnyakov⁶⁵, P. Pralavorio⁸⁵, A. Pranko¹⁵, S. Prasad³⁰, S. Prell⁶⁴, D. Price⁸⁴, L. E. Price⁶, M. Primavera^{73a}, S. Prince⁸⁷, M. Proissl⁴⁶, K. Prokofiev^{60c}, F. Prokoshin^{32b}, E. Protopapadaki¹³⁶, S. Protopopescu²⁵, J. Proudfoot⁶, M. Przybycien^{38a}, E. Ptacek¹¹⁶, D. Puddu^{134a,134b}, E. Pueschel⁸⁶, D. Poldon¹⁴⁸, M. Purohit^{25,ae}, P. Puzo¹¹⁷, J. Qian⁸⁹, G. Qin⁵³, Y. Qin⁸⁴, A. Quadt⁵⁴, D. R. Quarrie¹⁵, W. B. Quayle^{164a,164b}, M. Queitsch-Maitland⁸⁴, D. Quilty⁵³, S. Raddum¹¹⁹, V. Radeka²⁵, V. Radescu⁴², S. K. Radhakrishnan¹⁴⁸, P. Radloff¹¹⁶, P. Rados⁸⁸, F. Ragusa^{91a,91b}, G. Rahal¹⁷⁸, S. Rajagopalan²⁵, M. Rammensee³⁰, C. Rangel-Smith¹⁶⁶, F. Rauscher¹⁰⁰, S. Rave⁸³, T. Ravenscroft⁵³, M. Raymond³⁰, A. L. Read¹¹⁹, N. P. Readioff⁷⁴, D. M. Rebuffi^{121a,121b}, A. Redelbach¹⁷⁴, G. Redlinger²⁵, R. Reece¹³⁷, K. Reeves⁴¹, L. Rehnisch¹⁶, J. Reichert¹²², H. Reisin²⁷, M. Relich¹⁶³, C. Rembser³⁰, H. Ren^{33a}, A. Renaud¹¹⁷, M. Rescigno^{132a}, S. Resconi^{91a}, O. L. Rezanova^{109,c}, P. Reznicek¹²⁹, R. Rezvani⁹⁵, R. Richter¹⁰¹, S. Richter⁷⁸, E. Richter-Was^{38b}, O. Ricken²¹, M. Ridel⁸⁰, P. Rieck¹⁶, C. J. Riegel¹⁷⁵, J. Rieger⁵⁴, O. Rifki¹¹³, M. Rijssenbeek¹⁴⁸, A. Rimoldi^{121a,121b}, L. Rinaldi^{20a}, B. Ristić⁴⁹, E. Ritsch³⁰, I. Riu¹², F. Rizatdinova¹¹⁴, E. Rizvi⁷⁶, S. H. Robertson^{87,k}, A. Robichaud-Veronneau⁸⁷, D. Robinson²⁸, J. E. M. Robinson⁴², A. Robson⁵³, C. Roda^{124a,124b}, S. Roe³⁰, O. Røhne¹¹⁹, S. Rolli¹⁶¹, A. Romaniouk⁹⁸, M. Romano^{20a,20b}, S. M. Romano Saez³⁴, E. Romero Adam¹⁶⁷, N. Rompotis¹³⁸, M. Ronzani⁴⁸, L. Roos⁸⁰, E. Ros¹⁶⁷, S. Rosati^{132a}, K. Rosbach⁴⁸, P. Rose¹³⁷, P. L. Rosendahl¹⁴, O. Rosenthal¹⁴¹, V. Rossetti^{146a,146b}, E. Rossi^{104a,104b}, L. P. Rossi^{50a}, J. H. N. Rosten²⁸, R. Rosten¹³⁸, M. Rotaru^{26b}, I. Roth¹⁷², J. Rothberg¹³⁸, D. Rousseau¹¹⁷, C. R. Royon¹³⁶, A. Rozanov⁸⁵, Y. Rozen¹⁵², X. Ruan^{145c}, F. Rubbo¹⁴³, I. Rubinskiy⁴², V. I. Rud⁹⁹, C. Rudolph⁴⁴, M. S. Rudolph¹⁵⁸, F. Rühr⁴⁸, A. Ruiz-Martinez³⁰, Z. Rurikova⁴⁸, N. A. Rusakovich⁶⁵, A. Ruschke¹⁰⁰, H. L. Russell¹³⁸, J. P. Rutherford⁷, N. Ruthmann⁴⁸, Y. F. Ryabov¹²³, M. Rybar¹⁶⁵, G. Rybkin¹¹⁷, N. C. Ryder¹²⁰, A. F. Saavedra¹⁵⁰, G. Sabato¹⁰⁷, S. Sacerdoti²⁷, A. Saddique³, H. F.-W. Sadrozinski¹³⁷, R. Sadykov⁶⁵, F. Safai Tehrani^{132a}, M. Sahinsoy^{58a}, M. Saimpert¹³⁶, T. Saito¹⁵⁵, H. Sakamoto¹⁵⁵, Y. Sakurai¹⁷¹, G. Salamanna^{134a,134b}, A. Salamon^{133a}, J. E. Salazar Loyola^{32b}, M. Saleem¹¹³, D. Salek¹⁰⁷, P. H. Sales De Bruin¹³⁸, D. Salihagic¹⁰¹, A. Salnikov¹⁴³, J. Salt¹⁶⁷, D. Salvatore^{37a,37b}, F. Salvatore¹⁴⁹, A. Salvucci^{60a}, A. Salzburger³⁰, D. Sammel⁴⁸, D. Sampsonidis¹⁵⁴, A. Sanchez^{104a,104b}, J. Sánchez¹⁶⁷, V. Sanchez Martinez¹⁶⁷, H. Sandaker¹¹⁹, R. L. Sandbach⁷⁶, H. G. Sander⁸³, M. P. Sanders¹⁰⁰, M. Sandhoff¹⁷⁵, C. Sandoval¹⁶², R. Sandstroem¹⁰¹, D. P. C. Sankey¹³¹

M. Sannino^{50a,50b}, A. Sansoni⁴⁷, C. Santoni³⁴, R. Santonico^{133a,133b}, H. Santos^{126a}, I. Santoyo Castillo¹⁴⁹, K. Sapp¹²⁵, A. Saproinov⁶⁵, J. G. Saraiva^{126a,126d}, B. Sarrazin²¹, O. Sasaki⁶⁶, Y. Sasaki¹⁵⁵, K. Sato¹⁶⁰, G. Sauvage^{5,*}, E. Sauvan⁵, G. Savage⁷⁷, P. Savard^{158,d}, C. Sawyer¹³¹, L. Sawyer^{79,n}, J. Saxon³¹, C. Sbarra^{20a}, A. Sbrizzi^{20a,20b}, T. Scanlon⁷⁸, D. A. Scannicchio¹⁶³, M. Scarcella¹⁵⁰, V. Scarfone^{37a,37b}, J. Schaarschmidt¹⁷², P. Schacht¹⁰¹, D. Schaefer³⁰, R. Schaefer⁴², J. Schaeffer⁸³, S. Schaepe²¹, S. Schaetzel^{58b}, U. Schäfer⁸³, A. C. Schaffer¹¹⁷, D. Schaile¹⁰⁰, R. D. Schamberger¹⁴⁸, V. Scharf^{58a}, V. A. Schegelsky¹²³, D. Scheirich¹²⁹, M. Schernau¹⁶³, C. Schiavi^{50a,50b}, C. Schillo⁴⁸, M. Schioppa^{37a,37b}, S. Schlenker³⁰, K. Schmieden³⁰, C. Schmitt⁸³, S. Schmitt^{58b}, S. Schmitt⁴², B. Schneider^{159a}, Y. J. Schnellbach⁷⁴, U. Schnoor⁴⁴, L. Schoeffel¹³⁶, A. Schoening^{58b}, B. D. Schoenrock⁹⁰, E. Schopf²¹, A. L. S. Schorlemmer⁵⁴, M. Schott⁸³, D. Schouten^{159a}, J. Schovancova⁸, S. Schramm⁴⁹, M. Schreyer¹⁷⁴, C. Schroeder⁸³, N. Schuh⁸³, M. J. Schultens²¹, H.-C. Schultz-Coulon^{58a}, H. Schulz¹⁶, M. Schumacher⁴⁸, B. A. Schumm¹³⁷, Ph. Schune¹³⁶, C. Schwanenberger⁸⁴, A. Schwartzman¹⁴³, T. A. Schwarz⁸⁹, Ph. Schwegler¹⁰¹, H. Schweiger⁸⁴, Ph. Schwemling¹³⁶, R. Schwienhorst⁹⁰, J. Schwindling¹³⁶, T. Schwindt²¹, F. G. Sciacca¹⁷, E. Scifo¹¹⁷, G. Sciolla²³, F. Scuri^{124a,124b}, F. Scutti²¹, J. Searcy⁸⁹, G. Sedov⁴², E. Sedykh¹²³, P. Seema²¹, S. C. Seidel¹⁰⁵, A. Seiden¹³⁷, F. Seifert¹²⁸, J. M. Seixas^{24a}, G. Sekhniaidze^{104a}, K. Sekhon⁸⁹, S. J. Sekula⁴⁰, D. M. Seliverstov^{123,*}, N. Semprini-Cesari^{20a,20b}, C. Serfon³⁰, L. Serin¹¹⁷, L. Serkin^{164a,164b}, T. Serre⁸⁵, M. Sessa^{134a,134b}, R. Seuster^{159a}, H. Severini¹¹³, T. Sfiligoj⁷⁵, F. Sforza³⁰, A. Sfyrla³⁰, E. Shabalina⁵⁴, M. Shamim¹¹⁶, L. Y. Shan^{33a}, R. Shang¹⁶⁵, J. T. Shank²², M. Shapiro¹⁵, P. B. Shatalov⁹⁷, K. Shaw^{164a,164b}, S. M. Shaw⁸⁴, A. Shcherbakova^{146a,146b}, C. Y. Shehu¹⁴⁹, P. Sherwood⁷⁸, L. Shi^{151.af}, S. Shimizu⁶⁷, C. O. Shimmin¹⁶³, M. Shimojima¹⁰², M. Shiyakova⁶⁵, A. Shmeleva⁹⁶, D. Shoaleh Saadi⁹⁵, M. J. Shochet³¹, S. Shojaii^{91a,91b}, S. Shrestha¹¹¹, E. Shulga⁹⁸, M. A. Shupe⁷, S. Shushkevich⁴², P. Sicho¹²⁷, P. E. Sidebo¹⁴⁷, O. Sidiropoulou¹⁷⁴, D. Sidorov¹¹⁴, A. Sidoti^{20a,20b}, F. Siegert⁴⁴, Dj. Sijacki¹³, J. Silva^{126a,126d}, Y. Silver¹⁵³, S. B. Silverstein^{146a}, V. Simak¹²⁸, O. Simard⁵, Lj. Simic¹³, S. Simion¹¹⁷, E. Simioni⁸³, B. Simmons⁷⁸, D. Simon³⁴, P. Sinervo¹⁵⁸, N. B. Sinev¹¹⁶, M. Sioli^{20a,20b}, G. Siragusa¹⁷⁴, A. N. Sisakyan^{65,*}, S. Yu. Sivoklov⁹⁹, J. Sjölin^{146a,146b}, T. B. Sjursen¹⁴, M. B. Skinner⁷², H. P. Skottowe⁵⁷, P. Skubic¹¹³, M. Slater¹⁸, T. Slavicek¹²⁸, M. Slawinska¹⁰⁷, K. Sliwa¹⁶¹, V. Smakhtin¹⁷², B. H. Smart⁴⁶, L. Smestad¹⁴, S. Yu. Smirnov⁹⁸, Y. Smirnov⁹⁸, L. N. Smirnova^{99.ag}, O. Smirnova⁸¹, M. N. K. Smith³⁵, R. W. Smith³⁵, M. Smizanska⁷², K. Smolek¹²⁸, A. A. Snesarev⁹⁶, G. Snidero⁷⁶, S. Snyder²⁵, R. Sobie^{169.k}, F. Socher⁴⁴, A. Soffer¹⁵³, D. A. Soh^{151.af}, G. Sokhranyii⁷⁵, C. A. Solans³⁰, M. Solar¹²⁸, J. Solc¹²⁸, E. Yu. Soldatov⁹⁸, U. Soldevila¹⁶⁷, A. A. Solodkov¹³⁰, A. Soloshenko⁶⁵, O. V. Solovyanov¹³⁰, V. Solovye¹²³, P. Sommer⁴⁸, H. Y. Song^{33b}, N. Soni¹, A. Sood¹⁵, A. Sopczak¹²⁸, B. Sopko¹²⁸, V. Sopko¹²⁸, V. Sorin¹², D. Sosa^{58b}, M. Sosebee⁸, C. L. Sotiropoulou^{124a,124b}, R. Soualah^{164a,164c}, A. M. Soukharev^{109.c}, D. South⁴², B. C. Sowden⁷⁷, S. Spagnolo^{73a,73b}, M. Spalla^{124a,124b}, M. Spangenberg¹⁷⁰, F. Spanò⁷⁷, W. R. Spearman⁵⁷, D. Sperlich¹⁶, F. Spettel¹⁰¹, R. Spighi^{20a}, G. Spigo³⁰, L. A. Spiller⁸⁸, M. Spousta¹²⁹, T. Spreitzer¹⁵⁸, R. D. St. Denis^{53,*}, A. Stabile^{91a}, S. Staerz⁴⁴, J. Stahlman¹²², R. Stamen^{58a}, S. Stamm¹⁶, E. Stanecka³⁹, C. Stanescu^{134a}, M. Stanescu-Bellu⁴², M. M. Stanitzki⁴², S. Stapnes¹¹⁹, E. A. Starchenko¹³⁰, J. Stark⁵⁵, P. Staroba¹²⁷, P. Starovoitov^{58a}, R. Staszewski³⁹, P. Steinberg²⁵, B. Stelzer¹⁴², H. J. Stelzer³⁰, O. Stelzer-Chilton^{159a}, H. Stenzel⁵², G. A. Stewart⁵³, J. A. Stillings²¹, M. C. Stockton⁸⁷, M. Stoebe⁸⁷, G. Stoicea^{26b}, P. Stolte⁵⁴, S. Stonjek¹⁰¹, A. R. Stradling⁸, A. Straessner⁴⁴, M. E. Stramaglia¹⁷, J. Strandberg¹⁴⁷, S. Strandberg^{146a,146b}, A. Strandlie¹¹⁹, E. Strauss¹⁴³, M. Strauss¹¹³, P. Strizenc^{144b}, R. Ströhmer¹⁷⁴, D. M. Strom¹¹⁶, R. Stroynowski⁴⁰, A. Strubig¹⁰⁶, S. A. Stucci¹⁷, B. Stugu¹⁴, N. A. Styles⁴², D. Su¹⁴³, J. Su¹²⁵, R. Subramaniam⁷⁹, A. Succurro¹², Y. Sugaya¹¹⁸, M. Suk¹²⁸, V. V. Sulin⁹⁶, S. Sultansoy^{4c}, T. Sumida⁶⁸, S. Sun⁵⁷, X. Sun^{33a}, J. E. Sundermann⁴⁸, K. Suruliz¹⁴⁹, G. Susinno^{37a,37b}, M. R. Sutton¹⁴⁹, S. Suzuki⁶⁶, M. Svatos¹²⁷, M. Swiatlowski¹⁴³, I. Sykora^{144a}, T. Sykora¹²⁹, D. Ta⁴⁸, C. Taccini^{134a,134b}, K. Tackmann⁴², J. Taenzer¹⁵⁸, A. Taffard¹⁶³, R. Tahirout^{159a}, N. Taiblum¹⁵³, H. Takai²⁵, R. Takashima⁶⁹, H. Takeda⁶⁷, T. Takeshita¹⁴⁰, Y. Takubo⁶⁶, M. Talby⁸⁵, A. A. Talyshev^{109.c}, J. Y. C. Tam¹⁷⁴, K. G. Tan⁸⁸, J. Tanaka¹⁵⁵, R. Tanaka¹¹⁷, S. Tanaka⁶⁶, B. B. Tannenwald¹¹¹, N. Tannoury²¹, S. Tapprogge⁸³, S. Tarem¹⁵², F. Tarrade²⁹, G. F. Tartarelli^{91a}, P. Tas¹²⁹, M. Tasevsky¹²⁷, T. Tashiro⁶⁸, E. Tassi^{37a,37b}, A. Tavares Delgado^{126a,126b}, Y. Tayalati^{135d}, F. E. Taylor⁹⁴, G. N. Taylor⁸⁸, P. T. E. Taylor⁸⁸, W. Taylor^{159b}, F. A. Teischinger³⁰, M. Teixeira Dias Castanheira⁷⁶, P. Teixeira-Dias⁷⁷, K. K. Temming⁴⁸, D. Temple¹⁴², H. Ten Kate³⁰, P. K. Teng¹⁵¹, J. J. Teoh¹¹⁸, F. Tepel¹⁷⁵, S. Terada⁶⁶, K. Terashi¹⁵⁵, J. Terron⁸², S. Terzo¹⁰¹, M. Testa⁴⁷, R. J. Teuscher^{158,k}, T. Theveneaux-Pelzer³⁴, J. P. Thomas¹⁸, J. Thomas-Wilsker⁷⁷, E. N. Thompson³⁵, P. D. Thompson¹⁸, R. J. Thompson⁸⁴, A. S. Thompson⁵³, L. A. Thomsen¹⁷⁶, E. Thomson¹²², M. Thomson²⁸, R. P. Thun^{89,*}, M. J. Tibbetts¹⁵, R. E. Tise Torres⁸⁵, V. O. Tikhomirov^{96.ah}, Yu. A. Tikhonov^{109.c}, S. Timoshenko⁹⁸, E. Tiouchichine⁸⁵, P. Tipton¹⁷⁶, S. Tisserant⁸⁵, K. Todome¹⁵⁷, T. Todorov^{5,*}, S. Todorova-Nova¹²⁹, J. Tojo⁷⁰, S. Tokár^{144a}, K. Tokushuku⁶⁶, K. Tollefson⁹⁰, E. Tolley⁵⁷, L. Tomlinson⁸⁴, M. Tomoto¹⁰³, L. Tompkins^{143.ai}, K. Toms¹⁰⁵, E. Torrence¹¹⁶, H. Torres¹⁴², E. Torró Pastor¹³⁸, J. Toth^{85.aj}, F. Touchard⁸⁵, D. R. Tovey¹³⁹, T. Trefzger¹⁷⁴, L. Tremblet³⁰, A. Tricoli³⁰, I. M. Trigger^{159a}, S. Trincaz-Duvold⁸⁰, M. F. Tripiana¹², W. Trischuk¹⁵⁸, B. Trocme⁵⁵, C. Troncon^{91a}, M. Trottier-McDonald¹⁵, M. Trovatelli¹⁶⁹, L. Truong^{164a,164c}, M. Trzebinski³⁹, A. Trzupek³⁹, C. Tsarouchas³⁰, J. C.-L. Tseng¹²⁰, P. V. Tsiarehka⁹²

D. Tsionou¹⁵⁴, G. Tsipolitis¹⁰, N. Tsirintanis⁹, S. Tsiskaridze¹², V. Tsiskaridze⁴⁸, E. G. Tskhadadze^{51a}, I. I. Tsukerman⁹⁷, V. Tsulaia¹⁵, S. Tsuno⁶⁶, D. Tsybychev¹⁴⁸, A. Tudorache^{26b}, V. Tudorache^{26b}, A. N. Tuna⁵⁷, S. A. Tupputi^{20a,20b}, S. Turchikhin^{99,ag}, D. Turecek¹²⁸, R. Turra^{91a,91b}, A. J. Turvey⁴⁰, P. M. Tuts³⁵, A. Tykhonov⁴⁹, M. Tylmad^{146a,146b}, M. Tyndel¹³¹, I. Ueda¹⁵⁵, R. Ueno²⁹, M. Ughetto^{146a,146b}, M. Ugland¹⁴, F. Ukegawa¹⁶⁰, G. Unal³⁰, A. Undrus²⁵, G. Unel¹⁶³, F. C. Ungaro⁴⁸, Y. Unno⁶⁶, C. Unverdorben¹⁰⁰, J. Urban^{144b}, P. Urquijo⁸⁸, P. Urrejola⁸³, G. Usai⁸, A. Usanova⁶², L. Vacavant⁸⁵, V. Vacek¹²⁸, B. Vachon⁸⁷, C. Valderanis⁸³, N. Valencic¹⁰⁷, S. Valentineti^{20a,20b}, A. Valero¹⁶⁷, L. Valery¹², S. Valkar¹²⁹, E. Valladolid Gallego¹⁶⁷, S. Vallecorsa⁴⁹, J. A. Valls Ferrer¹⁶⁷, W. Van Den Wollenberg¹⁰⁷, P. C. Van Der Deijl¹⁰⁷, R. van der Geer¹⁰⁷, H. van der Graaf¹⁰⁷, N. van Eldik¹⁵², P. van Gemmeren⁶, J. Van Nieuwkoop¹⁴², I. van Vulpen¹⁰⁷, M. C. van Woerden³⁰, M. Vanadia^{132a,132b}, W. Vandelli³⁰, R. Vanguri¹²², A. Vaniachine⁶, F. Vannucci⁸⁰, G. Vardanyan¹⁷⁷, R. Vari^{132a}, E. W. Varnes⁷, T. Varol⁴⁰, D. Varouchas⁸⁰, A. Vartapetian⁸, K. E. Varvell¹⁵⁰, F. Vazeille³⁴, T. Vazquez Schroeder⁸⁷, J. Veatch⁷, L. M. Veloce¹⁵⁸, F. Veloso^{126a,126c}, T. Velz²¹, S. Veneziano^{132a}, A. Ventura^{73a,73b}, D. Ventura⁸⁶, M. Venturi¹⁶⁹, N. Venturi¹⁵⁸, A. Venturini²³, V. Vercesi^{121a}, M. Verducci^{132a,132b}, W. Verkerke¹⁰⁷, J. C. Vermeulen¹⁰⁷, A. Vest⁴⁴, M. C. Vetterli^{142,d}, O. Viazlo⁸¹, I. Vichou¹⁶⁵, T. Vickey¹³⁹, O. E. Vickey Boeriu¹³⁹, G. H. A. Viehhauser¹²⁰, S. Viel¹⁵, R. Vigne⁶², M. Villa^{20a,20b}, M. Villaplana Perez^{91a,91b}, E. Vilucchi⁴⁷, M. G. Vincet²⁹, V. B. Vinogradov⁶⁵, I. Vivarelli¹⁴⁹, F. Vives Vaque³, S. Vlachos¹⁰, D. Vladioiu¹⁰⁰, M. Vlasak¹²⁸, M. Vogel^{32a}, P. Vokac¹²⁸, G. Volpi^{124a,124b}, M. Volpi⁸⁸, H. von der Schmitt¹⁰¹, H. von Radziewski⁴⁸, E. von Toerne²¹, V. Vorobel¹²⁹, K. Vorobev⁹⁸, M. Vos¹⁶⁷, R. Voss³⁰, J. H. Vosseveld⁷⁴, N. Vranjes¹³, M. Vranjes Milosavljevic¹³, V. Vrba¹²⁷, M. Vreeswijk¹⁰⁷, R. Vuillemet³⁰, I. Vukotic³¹, Z. Vykydal¹²⁸, P. Wagner²¹, W. Wagner¹⁷⁵, H. Wahlberg⁷¹, S. Wahrmund⁴⁴, J. Wakabayashi¹⁰³, J. Walder⁷², R. Walker¹⁰⁰, W. Walkowiak¹⁴¹, C. Wang¹⁵¹, F. Wang¹⁷³, H. Wang¹⁵, H. Wang⁴⁰, J. Wang⁴², J. Wang¹⁵⁰, K. Wang⁸⁷, R. Wang⁶, S. M. Wang¹⁵¹, T. Wang²¹, T. Wang³⁵, X. Wang¹⁷⁶, C. Wanotayaroj¹¹⁶, A. Warburton⁸⁷, C. P. Ward²⁸, D. R. Wardrope⁷⁸, A. Washbrook⁴⁶, C. Wasicki⁴², P. M. Watkins¹⁸, A. T. Watson¹⁸, I. J. Watson¹⁵⁰, M. F. Watson¹⁸, G. Watts¹³⁸, S. Watts⁸⁴, B. M. Waugh⁷⁸, S. Webb⁸⁴, M. S. Weber¹⁷, S. W. Weber¹⁷⁴, J. S. Webster³¹, A. R. Weidberg¹²⁰, B. Weinert⁶¹, J. Weingarten⁵⁴, C. Weiser⁴⁸, H. Weits¹⁰⁷, P. S. Wells³⁰, T. Wenaus²⁵, T. Wengler³⁰, S. Wenig³⁰, N. Wermes²¹, M. Werner⁴⁸, P. Werner³⁰, M. Wessels^{58a}, J. Wetter¹⁶¹, K. Whalen¹¹⁶, A. M. Wharton⁷², A. White⁸, M. J. White¹, R. White^{32b}, S. White^{124a,124b}, D. Whiteson¹⁶³, F. J. Wickens¹³¹, W. Wiedenmann¹⁷³, M. Wielers¹³¹, P. Wienemann²¹, C. Wiglesworth³⁶, L. A. M. Wiik-Fuchs²¹, A. Wildauer¹⁰¹, H. G. Wilkens³⁰, H. H. Williams¹²², S. Williams¹⁰⁷, C. Willis⁹⁰, S. Willocq⁸⁶, A. Wilson⁸⁹, J. A. Wilson¹⁸, I. Wingerter-Seez⁵, F. Winklmeier¹¹⁶, B. T. Winter²¹, M. Wittgen¹⁴³, J. Wittkowski¹⁰⁰, S. J. Wollstadt⁸³, M. W. Wolter³⁹, H. Wolters^{126a,126c}, B. K. Wosiek³⁹, J. Wotschack³⁰, M. J. Woudstra⁸⁴, K. W. Wozniak³⁹, M. Wu⁵⁵, M. Wu³¹, S. L. Wu¹⁷³, X. Wu⁴⁹, Y. Wu⁸⁹, T. R. Wyatt⁸⁴, B. M. Wynne⁴⁶, S. Xella³⁶, D. Xu^{33a}, L. Xu²⁵, B. Yabsley¹⁵⁰, S. Yacoub^{145a}, R. Yakabe⁶⁷, M. Yamada⁶⁶, D. Yamaguchi¹⁵⁷, Y. Yamaguchi¹¹⁸, A. Yamamoto⁶⁶, S. Yamamoto¹⁵⁵, T. Yamanaka¹⁵⁵, K. Yamauchi¹⁰³, Y. Yamazaki⁶⁷, Z. Yan²², H. Yang^{33e}, H. Yang¹⁷³, Y. Yang¹⁵¹, W-M. Yao¹⁵, Y. Yasu⁶⁶, E. Yatsenko⁵, K. H. Yau Wong²¹, J. Ye⁴⁰, S. Ye²⁵, I. Yeletsikh⁶⁵, A. L. Yen⁵⁷, E. Yildirim⁴², K. Yorita¹⁷¹, R. Yoshida⁶, K. Yoshihara¹²², C. Young¹⁴³, C. J. S. Young³⁰, S. Youssef²², D. R. Yu¹⁵, J. Yu⁸, J. M. Yu⁸⁹, J. Yu¹¹⁴, L. Yuan⁶⁷, S. P. Y. Yuen²¹, A. Yurkewicz¹⁰⁸, I. Yusuff^{28,ak}, B. Zabinski³⁹, R. Zaidan⁶³, A. M. Zaitsev^{130,ab}, J. Zalieckas¹⁴, A. Zaman¹⁴⁸, S. Zambito⁵⁷, L. Zanello^{132a,132b}, D. Zanzi⁸⁸, C. Zeitnitz¹⁷⁵, M. Zeman¹²⁸, A. Zemla^{38a}, Q. Zeng¹⁴³, K. Zengel²³, O. Zenin¹³⁰, T. Ženiš^{144a}, D. Zerwas¹¹⁷, D. Zhang⁸⁹, F. Zhang¹⁷³, H. Zhang^{33c}, J. Zhang⁶, L. Zhang⁴⁸, R. Zhang^{33b}, X. Zhang^{33d}, Z. Zhang¹¹⁷, X. Zhao⁴⁰, Y. Zhao^{33d,117}, Z. Zhao^{33b}, A. Zhemchugov⁶⁵, J. Zhong¹²⁰, B. Zhou⁸⁹, C. Zhou⁴⁵, L. Zhou³⁵, L. Zhou⁴⁰, M. Zhou¹⁴⁸, N. Zhou^{33f}, C. G. Zhu^{33d}, H. Zhu^{33a}, J. Zhu⁸⁹, Y. Zhu^{33b}, X. Zhuang^{33a}, K. Zhukov⁹⁶, A. Zibell¹⁷⁴, D. Zieminska⁶¹, N. I. Zimine⁶⁵, C. Zimmermann⁸³, S. Zimmermann⁴⁸, Z. Zinonos⁵⁴, M. Zinser⁸³, M. Ziolkowski¹⁴¹, L. Živković¹³, G. Zobernig¹⁷³, A. Zoccoli^{20a,20b}, M. zur Nedden¹⁶, G. Zurzolo^{104a,104b}, L. Zwalinski³⁰

¹ Department of Physics, University of Adelaide, Adelaide, Australia

² Physics Department, SUNY Albany, Albany, NY, USA

³ Department of Physics, University of Alberta, Edmonton, AB, Canada

⁴ (a)Department of Physics, Ankara University, Ankara, Turkey; (b)Istanbul Aydin University, Istanbul, Turkey;

(c)Division of Physics, TOBB University of Economics and Technology, Ankara, Turkey

⁵ LAPP, CNRS/IN2P3 and Université Savoie Mont Blanc, Annecy-le-Vieux, France

⁶ High Energy Physics Division, Argonne National Laboratory, Argonne, IL, USA

⁷ Department of Physics, University of Arizona, Tucson, AZ, USA

⁸ Department of Physics, The University of Texas at Arlington, Arlington, TX, USA

⁹ Physics Department, University of Athens, Athens, Greece

¹⁰ Physics Department, National Technical University of Athens, Zografou, Greece

- 11 Institute of Physics, Azerbaijan Academy of Sciences, Baku, Azerbaijan
- 12 Institut de Física d'Altes Energies and Departament de Física de la Universitat Autònoma de Barcelona, Barcelona, Spain
- 13 Institute of Physics, University of Belgrade, Belgrade, Serbia
- 14 Department for Physics and Technology, University of Bergen, Bergen, Norway
- 15 Physics Division, Lawrence Berkeley National Laboratory and University of California, Berkeley, CA, USA
- 16 Department of Physics, Humboldt University, Berlin, Germany
- 17 Albert Einstein Center for Fundamental Physics and Laboratory for High Energy Physics, University of Bern, Bern, Switzerland
- 18 School of Physics and Astronomy, University of Birmingham, Birmingham, UK
- 19 (a)Department of Physics, Bogazici University, Istanbul, Turkey; (b)Department of Physics Engineering, Gaziantep University, Gaziantep, Turkey; (c)Department of Physics, Dogus University, Istanbul, Turkey
- 20 (a)INFN Sezione di Bologna, Bologna, Italy; (b)Dipartimento di Fisica e Astronomia, Università di Bologna, Bologna, Italy
- 21 Physikalisches Institut, University of Bonn, Bonn, Germany
- 22 Department of Physics, Boston University, Boston, MA, USA
- 23 Department of Physics, Brandeis University, Waltham, MA, USA
- 24 (a)Universidade Federal do Rio De Janeiro COPPE/EE/IF, Rio de Janeiro, Brazil; (b)Electrical Circuits Department, Federal University of Juiz de Fora (UFJF), Juiz de Fora, Brazil; (c)Federal University of Sao Joao del Rei (UFSJ), Sao Joao del Rei, Brazil; (d)Instituto de Fisica, Universidade de Sao Paulo, São Paulo, Brazil
- 25 Physics Department, Brookhaven National Laboratory, Upton, NY, USA
- 26 (a)Transilvania University of Brasov, Brasov, Romania; (b)National Institute of Physics and Nuclear Engineering, Bucharest, Romania; (c)Physics Department, National Institute for Research and Development of Isotopic and Molecular Technologies, Cluj Napoca, Romania; (d)University Politehnica Bucharest, Bucharest, Romania; (e)West University in Timisoara, Timisoara, Romania
- 27 Departamento de Física, Universidad de Buenos Aires, Buenos Aires, Argentina
- 28 Cavendish Laboratory, University of Cambridge, Cambridge, UK
- 29 Department of Physics, Carleton University, Ottawa, ON, Canada
- 30 CERN, Geneva, Switzerland
- 31 Enrico Fermi Institute, University of Chicago, Chicago, IL, USA
- 32 (a)Departamento de Física, Pontificia Universidad Católica de Chile, Santiago, Chile; (b)Departamento de Física, Universidad Técnica Federico Santa María, Valparaiso, Chile
- 33 (a)Institute of High Energy Physics, Chinese Academy of Sciences, Beijing, China; (b)Department of Modern Physics, University of Science and Technology of China, Hefei, Anhui, China; (c)Department of Physics, Nanjing University, Nanjing, Jiangsu, China; (d)School of Physics, Shandong University, Jinan, Shandong, China; (e)Shanghai Key Laboratory for Particle Physics and Cosmology, Department of Physics and Astronomy, Shanghai Jiao Tong University, Shanghai, China; (f)Physics Department, Tsinghua University, Beijing 100084, China
- 34 Laboratoire de Physique Corpusculaire, Clermont Université and Université Blaise Pascal and CNRS/IN2P3, Clermont-Ferrand, France
- 35 Nevis Laboratory, Columbia University, Irvington, NY, USA
- 36 Niels Bohr Institute, University of Copenhagen, Copenhagen, Denmark
- 37 (a)INFN Gruppo Collegato di Cosenza, Laboratori Nazionali di Frascati, Frascati, Italy; (b)Dipartimento di Fisica, Università della Calabria, Rende, Italy
- 38 (a)AGH University of Science and Technology, Faculty of Physics and Applied Computer Science, Kraków, Poland; (b)Marian Smoluchowski Institute of Physics, Jagiellonian University, Kraków, Poland
- 39 Institute of Nuclear Physics, Polish Academy of Sciences, Kraków, Poland
- 40 Physics Department, Southern Methodist University, Dallas, TX, USA
- 41 Physics Department, University of Texas at Dallas, Richardson, TX, USA
- 42 DESY, Hamburg and Zeuthen, Germany
- 43 Institut für Experimentelle Physik IV, Technische Universität Dortmund, Dortmund, Germany
- 44 Institut für Kern- und Teilchenphysik, Technische Universität Dresden, Dresden, Germany
- 45 Department of Physics, Duke University, Durham, NC, USA
- 46 SUPA - School of Physics and Astronomy, University of Edinburgh, Edinburgh, UK
- 47 INFN Laboratori Nazionali di Frascati, Frascati, Italy

- 48 Fakultät für Mathematik und Physik, Albert-Ludwigs-Universität, Freiburg, Germany
- 49 Section de Physique, Université de Genève, Geneva, Switzerland
- 50 ^(a)INFN Sezione di Genova, Genoa, Italy; ^(b)Dipartimento di Fisica, Università di Genova, Genoa, Italy
- 51 ^(a)E. Andronikashvili Institute of Physics, Iv. Javakishvili Tbilisi State University, Tbilisi, Georgia; ^(b)High Energy Physics Institute, Tbilisi State University, Tbilisi, Georgia
- 52 II Physikalisches Institut, Justus-Liebig-Universität Giessen, Giessen, Germany
- 53 SUPA - School of Physics and Astronomy, University of Glasgow, Glasgow, UK
- 54 II Physikalisches Institut, Georg-August-Universität, Göttingen, Germany
- 55 Laboratoire de Physique Subatomique et de Cosmologie, Université Grenoble-Alpes, CNRS/IN2P3, Grenoble, France
- 56 Department of Physics, Hampton University, Hampton, VA, USA
- 57 Laboratory for Particle Physics and Cosmology, Harvard University, Cambridge, MA, USA
- 58 ^(a)Kirchhoff-Institut für Physik, Ruprecht-Karls-Universität Heidelberg, Heidelberg, Germany; ^(b)Physikalisches Institut, Ruprecht-Karls-Universität Heidelberg, Heidelberg, Germany; ^(c)ZITI Institut für technische Informatik, Ruprecht-Karls-Universität Heidelberg, Mannheim, Germany
- 59 Faculty of Applied Information Science, Hiroshima Institute of Technology, Hiroshima, Japan
- 60 ^(a)Department of Physics, The Chinese University of Hong Kong, Shatin, NT, Hong Kong; ^(b)Department of Physics, The University of Hong Kong, Pokfulam, Hong Kong; ^(c)Department of Physics, The Hong Kong University of Science and Technology, Clear Water Bay, Kowloon, Hong Kong, China
- 61 Department of Physics, Indiana University, Bloomington, IN, USA
- 62 Institut für Astro- und Teilchenphysik, Leopold-Franzens-Universität, Innsbruck, Austria
- 63 University of Iowa, Iowa City, IA, USA
- 64 Department of Physics and Astronomy, Iowa State University, Ames, IA, USA
- 65 Joint Institute for Nuclear Research, JINR Dubna, Dubna, Russia
- 66 KEK, High Energy Accelerator Research Organization, Tsukuba, Japan
- 67 Graduate School of Science, Kobe University, Kobe, Japan
- 68 Faculty of Science, Kyoto University, Kyoto, Japan
- 69 Kyoto University of Education, Kyoto, Japan
- 70 Department of Physics, Kyushu University, Fukuoka, Japan
- 71 Instituto de Física La Plata, Universidad Nacional de La Plata and CONICET, La Plata, Argentina
- 72 Physics Department, Lancaster University, Lancaster, UK
- 73 ^(a)INFN Sezione di Lecce, Lecce, Italy; ^(b)Dipartimento di Matematica e Fisica, Università del Salento, Lecce, Italy
- 74 Oliver Lodge Laboratory, University of Liverpool, Liverpool, UK
- 75 Department of Physics, Jožef Stefan Institute and University of Ljubljana, Ljubljana, Slovenia
- 76 School of Physics and Astronomy, Queen Mary University of London, London, UK
- 77 Department of Physics, Royal Holloway University of London, Surrey, UK
- 78 Department of Physics and Astronomy, University College London, London, UK
- 79 Louisiana Tech University, Ruston, LA, USA
- 80 Laboratoire de Physique Nucléaire et de Hautes Energies, UPMC and Université Paris-Diderot and CNRS/IN2P3, Paris, France
- 81 Fysiska institutionen, Lunds universitet, Lund, Sweden
- 82 Departamento de Física Teórica C-15, Universidad Autónoma de Madrid, Madrid, Spain
- 83 Institut für Physik, Universität Mainz, Mainz, Germany
- 84 School of Physics and Astronomy, University of Manchester, Manchester, UK
- 85 CPPM, Aix-Marseille Université and CNRS/IN2P3, Marseille, France
- 86 Department of Physics, University of Massachusetts, Amherst, MA, USA
- 87 Department of Physics, McGill University, Montreal, QC, Canada
- 88 School of Physics, University of Melbourne, Victoria, Australia
- 89 Department of Physics, The University of Michigan, Ann Arbor, MI, USA
- 90 Department of Physics and Astronomy, Michigan State University, East Lansing, MI, USA
- 91 ^(a)INFN Sezione di Milano, Milan, Italy; ^(b)Dipartimento di Fisica, Università di Milano, Milan, Italy
- 92 B.I. Stepanov Institute of Physics, National Academy of Sciences of Belarus, Minsk, Republic of Belarus
- 93 National Scientific and Educational Centre for Particle and High Energy Physics, Minsk, Republic of Belarus
- 94 Department of Physics, Massachusetts Institute of Technology, Cambridge, MA, USA

- 95 Group of Particle Physics, University of Montreal, Montreal, QC, Canada
- 96 P.N. Lebedev Institute of Physics, Academy of Sciences, Moscow, Russia
- 97 Institute for Theoretical and Experimental Physics (ITEP), Moscow, Russia
- 98 National Research Nuclear University MEPhI, Moscow, Russia
- 99 D.V. Skobeltsyn Institute of Nuclear Physics, M.V. Lomonosov Moscow State University, Moscow, Russia
- 100 Fakultät für Physik, Ludwig-Maximilians-Universität München, Munich, Germany
- 101 Max-Planck-Institut für Physik (Werner-Heisenberg-Institut), München, Germany
- 102 Nagasaki Institute of Applied Science, Nagasaki, Japan
- 103 Graduate School of Science and Kobayashi-Maskawa Institute, Nagoya University, Nagoya, Japan
- 104 (a)INFN Sezione di Napoli, Naples, Italy; (b)Dipartimento di Fisica, Università di Napoli, Naples, Italy
- 105 Department of Physics and Astronomy, University of New Mexico, Albuquerque, NM, USA
- 106 Institute for Mathematics, Astrophysics and Particle Physics, Radboud University Nijmegen/Nikhef, Nijmegen, The Netherlands
- 107 Nikhef National Institute for Subatomic Physics and University of Amsterdam, Amsterdam, The Netherlands
- 108 Department of Physics, Northern Illinois University, De Kalb, IL, USA
- 109 Budker Institute of Nuclear Physics, SB RAS, Novosibirsk, Russia
- 110 Department of Physics, New York University, New York, NY, USA
- 111 Ohio State University, Columbus, OH, USA
- 112 Faculty of Science, Okayama University, Okayama, Japan
- 113 Homer L. Dodge Department of Physics and Astronomy, University of Oklahoma, Norman, OK, USA
- 114 Department of Physics, Oklahoma State University, Stillwater, OK, USA
- 115 Palacký University, RCPTM, Olomouc, Czech Republic
- 116 Center for High Energy Physics, University of Oregon, Eugene, OR, USA
- 117 LAL, Université Paris-Sud and CNRS/IN2P3, Orsay, France
- 118 Graduate School of Science, Osaka University, Osaka, Japan
- 119 Department of Physics, University of Oslo, Oslo, Norway
- 120 Department of Physics, Oxford University, Oxford, UK
- 121 (a)INFN Sezione di Pavia, Pavia, Italy; (b)Dipartimento di Fisica, Università di Pavia, Pavia, Italy
- 122 Department of Physics, University of Pennsylvania, Philadelphia, PA, USA
- 123 National Research Centre “Kurchatov Institute” B.P.Konstantinov Petersburg Nuclear Physics Institute, St. Petersburg, Russia
- 124 (a)INFN Sezione di Pisa, Pisa, Italy; (b)Dipartimento di Fisica E. Fermi, Università di Pisa, Pisa, Italy
- 125 Department of Physics and Astronomy, University of Pittsburgh, Pittsburgh, PA, USA
- 126 (a)Laboratório de Instrumentação e Física Experimental de Partículas-LIP, Lisbon, Portugal; (b)Faculdade de Ciências, Universidade de Lisboa, Lisbon, Portugal; (c)Department of Physics, University of Coimbra, Coimbra, Portugal; (d)Centro de Física Nuclear da Universidade de Lisboa, Lisbon, Portugal; (e)Departamento de Física, Universidade do Minho, Braga, Portugal; (f)Departamento de Física Teórica y del Cosmos and CAFPE, Universidad de Granada, Granada, Spain; (g)Dep Física and CEFITEC of Faculdade de Ciências e Tecnologia, Universidade Nova de Lisboa, Caparica, Portugal
- 127 Institute of Physics, Academy of Sciences of the Czech Republic, Prague, Czech Republic
- 128 Czech Technical University in Prague, Prague, Czech Republic
- 129 Faculty of Mathematics and Physics, Charles University in Prague, Prague, Czech Republic
- 130 State Research Center Institute for High Energy Physics, Protvino, Russia
- 131 Particle Physics Department, Rutherford Appleton Laboratory, Didcot, UK
- 132 (a)INFN Sezione di Roma, Rome, Italy; (b)Dipartimento di Fisica, Sapienza Università di Roma, Rome, Italy
- 133 (a)INFN Sezione di Roma Tor Vergata, Rome, Italy; (b)Dipartimento di Fisica, Università di Roma Tor Vergata, Rome, Italy
- 134 (a)INFN Sezione di Roma Tre, Rome, Italy; (b)Dipartimento di Matematica e Fisica, Università Roma Tre, Rome, Italy
- 135 (a)Faculté des Sciences Ain Chock, Réseau Universitaire de Physique des Hautes Energies-Université Hassan II, Casablanca, Morocco; (b)Centre National de l’Energie des Sciences Techniques Nucleaires, Rabat, Morocco; (c)Faculté des Sciences Semlalia, Université Cadi Ayyad, LPHEA-Marrakech, Marrakech, Morocco; (d)Faculté des Sciences, Université Mohamed Premier and LTPM, Oujda, Morocco; (e)Faculté des Sciences, Université Mohammed V, Rabat, Morocco

- 136 DSM/IRFU (Institut de Recherches sur les Lois Fondamentales de l'Univers), CEA Saclay (Commissariat à l'Énergie Atomique et aux Énergies Alternatives), Gif-sur-Yvette, France
- 137 Santa Cruz Institute for Particle Physics, University of California Santa Cruz, Santa Cruz, CA, USA
- 138 Department of Physics, University of Washington, Seattle, WA, USA
- 139 Department of Physics and Astronomy, University of Sheffield, Sheffield, UK
- 140 Department of Physics, Shinshu University, Nagano, Japan
- 141 Fachbereich Physik, Universität Siegen, Siegen, Germany
- 142 Department of Physics, Simon Fraser University, Burnaby, BC, Canada
- 143 SLAC National Accelerator Laboratory, Stanford, CA, USA
- 144 ^(a)Faculty of Mathematics, Physics and Informatics, Comenius University, Bratislava, Slovak Republic; ^(b)Department of Subnuclear Physics, Institute of Experimental Physics of the Slovak Academy of Sciences, Kosice, Slovak Republic
- 145 ^(a)Department of Physics, University of Cape Town, Cape Town, South Africa; ^(b)Department of Physics, University of Johannesburg, Johannesburg, South Africa; ^(c)School of Physics, University of the Witwatersrand, Johannesburg, South Africa
- 146 ^(a)Department of Physics, Stockholm University, Stockholm, Sweden; ^(b)The Oskar Klein Centre, Stockholm, Sweden
- 147 Physics Department, Royal Institute of Technology, Stockholm, Sweden
- 148 Departments of Physics and Astronomy and Chemistry, Stony Brook University, Stony Brook, NY, USA
- 149 Department of Physics and Astronomy, University of Sussex, Brighton, UK
- 150 School of Physics, University of Sydney, Sydney, Australia
- 151 Institute of Physics, Academia Sinica, Taipei, Taiwan
- 152 Department of Physics, Technion: Israel Institute of Technology, Haifa, Israel
- 153 Raymond and Beverly Sackler School of Physics and Astronomy, Tel Aviv University, Tel Aviv, Israel
- 154 Department of Physics, Aristotle University of Thessaloniki, Thessaloníki, Greece
- 155 International Center for Elementary Particle Physics and Department of Physics, The University of Tokyo, Tokyo, Japan
- 156 Graduate School of Science and Technology, Tokyo Metropolitan University, Tokyo, Japan
- 157 Department of Physics, Tokyo Institute of Technology, Tokyo, Japan
- 158 Department of Physics, University of Toronto, Toronto, ON, Canada
- 159 ^(a)TRIUMF, Vancouver, BC, Canada; ^(b)Department of Physics and Astronomy, York University, Toronto, ON, Canada
- 160 Faculty of Pure and Applied Sciences, University of Tsukuba, Tsukuba, Japan
- 161 Department of Physics and Astronomy, Tufts University, Medford, MA, USA
- 162 Centro de Investigaciones, Universidad Antonio Narino, Bogotá, Colombia
- 163 Department of Physics and Astronomy, University of California Irvine, Irvine, CA, USA
- 164 ^(a)INFN Gruppo Collegato di Udine, Sezione di Trieste, Udine, Italy; ^(b)ICTP, Trieste, Italy; ^(c)Dipartimento di Chimica Fisica e Ambiente, Università di Udine, Udine, Italy
- 165 Department of Physics, University of Illinois, Urbana, IL, USA
- 166 Department of Physics and Astronomy, University of Uppsala, Uppsala, Sweden
- 167 Instituto de Física Corpuscular (IFIC) and Departamento de Física Atómica, Molecular y Nuclear and Departamento de Ingeniería Electrónica and Instituto de Microelectrónica de Barcelona (IMB-CNM), University of Valencia and CSIC, Valencia, Spain
- 168 Department of Physics, University of British Columbia, Vancouver, BC, Canada
- 169 Department of Physics and Astronomy, University of Victoria, Victoria, BC, Canada
- 170 Department of Physics, University of Warwick, Coventry, UK
- 171 Waseda University, Tokyo, Japan
- 172 Department of Particle Physics, The Weizmann Institute of Science, Rehovot, Israel
- 173 Department of Physics, University of Wisconsin, Madison, WI, USA
- 174 Fakultät für Physik und Astronomie, Julius-Maximilians-Universität, Würzburg, Germany
- 175 Fachbereich C Physik, Bergische Universität Wuppertal, Wuppertal, Germany
- 176 Department of Physics, Yale University, New Haven, CT, USA
- 177 Yerevan Physics Institute, Yerevan, Armenia
- 178 Centre de Calcul de l'Institut National de Physique Nucléaire et de Physique des Particules (IN2P3), Villeurbanne, France

^a Also at Department of Physics, King's College London, London, UK

^b Also at Institute of Physics, Azerbaijan Academy of Sciences, Baku, Azerbaijan

- ^c Also at Novosibirsk State University, Novosibirsk, Russia
- ^d Also at TRIUMF, Vancouver, BC, Canada
- ^e Also at Department of Physics, California State University, Fresno, CA, USA
- ^f Also at Department of Physics, University of Fribourg, Fribourg, Switzerland
- ^g Also at Departamento de Fisica e Astronomia, Faculdade de Ciencias, Universidade do Porto, Porto, Portugal
- ^h Also at Tomsk State University, Tomsk, Russia
- ⁱ Also at CPPM, Aix-Marseille Université and CNRS/IN2P3, Marseille, France
- ^j Also at Università di Napoli Parthenope, Naples, Italy
- ^k Also at Institute of Particle Physics (IPP), Victoria, Canada
- ^l Also at Particle Physics Department, Rutherford Appleton Laboratory, Didcot, UK
- ^m Also at Department of Physics, St. Petersburg State Polytechnical University, St. Petersburg, Russia
- ⁿ Also at Louisiana Tech University, Ruston, LA, USA
- ^o Also at Institutio Catalana de Recerca i Estudis Avancats, ICREA, Barcelona, Spain
- ^p Also at Graduate School of Science, Osaka University, Osaka, Japan
- ^q Also at Department of Physics, National Tsing Hua University, Taiwan
- ^r Also at Department of Physics, The University of Texas at Austin, Austin, TX, USA
- ^s Also at Institute of Theoretical Physics, Ilia State University, Tbilisi, Georgia
- ^t Also at CERN, Geneva, Switzerland
- ^u Also at Georgian Technical University (GTU), Tbilisi, Georgia
- ^v Also at Manhattan College, New York, NY, USA
- ^w Also at Hellenic Open University, Patras, Greece
- ^x Also at Institute of Physics, Academia Sinica, Taipei, Taiwan
- ^y Also at LAL, Université Paris-Sud and CNRS/IN2P3, Orsay, France
- ^z Also at Academia Sinica Grid Computing, Institute of Physics, Academia Sinica, Taipei, Taiwan
- ^{aa} Also at School of Physics, Shandong University, Shandong, China
- ^{ab} Also at Moscow Institute of Physics and Technology State University, Dolgoprudny, Russia
- ^{ac} Also at Section de Physique, Université de Genève, Geneva, Switzerland
- ^{ad} Also at International School for Advanced Studies (SISSA), Trieste, Italy
- ^{ae} Also at Department of Physics and Astronomy, University of South Carolina, Columbia, SC, USA
- ^{af} Also at School of Physics and Engineering, Sun Yat-sen University, Guangzhou, China
- ^{ag} Also at Faculty of Physics, M.V. Lomonosov Moscow State University, Moscow, Russia
- ^{ah} Also at National Research Nuclear University MEPhI, Moscow, Russia
- ^{ai} Also at Department of Physics, Stanford University, Stanford, CA, USA
- ^{aj} Also at Institute for Particle and Nuclear Physics, Wigner Research Centre for Physics, Budapest, Hungary
- ^{ak} Also at University of Malaya, Department of Physics, Kuala Lumpur, Malaysia
- * Deceased